AGU PUBLICATIONS

Tectonics

RESEARCH ARTICLE
10.1002/2015TC003886

Key Points:
- Architecture of a hyperslow oceanic rift is deduced from Sao Miguel Island
- Rifting is concentrated at the master faults bounding the Terceira Rift (TR)
- N80 trend of Sao Miguel follows a transform between two major TR segments

Supporting Information:
- Figures S1–S5 and Data Set S1
- Data Set S1

Correspondence to:
A. L. R. Sibrant,
aurore.sibrant@u-psud.fr

Citation:
Sibrant, A. L. R., F. O. Marques, A. Hildenbrand, T. Boulesteix, A. C. G. Costa, and J. Catalão (2016), Deformation in a hyperslow oceanic rift: Insights from the tectonics of the São Miguel Island (Terceira Rift, Azores), *Tectonics*, *35*, 425–446, doi:10.1002/2015TC003886.

Received 25 MAR 2015
Accepted 26 JAN 2016
Accepted article online 29 JAN 2016
Published online 25 FEB 2016

Deformation in a hyperslow oceanic rift: Insights from the tectonics of the São Miguel Island (Terceira Rift, Azores)

A. L. R. Sibrant[1,2], F. O. Marques[3], A. Hildenbrand[1], T. Boulesteix[4], A. C. G. Costa[1,5], and J. Catalão[5]

[1]GEOPS, Université Paris-Sud, CNRS, Université Paris-Saclay, Orsay, France, [2]Now at Laboratoire FAST, Université Paris-Sud, CNRS, Université Paris-Saclay, Orsay, France, [3]Universidade de Lisboa, Lisboa, Portugal, [4]GeoRessources, CNRS-CREGU, Université de Lorraine, Nancy, France, [5]University of Lisbon and IDL, Lisbon, Portugal

Abstract The evolution of hyperslow oceanic rifts, like the Terceira Rift (TR) in the Azores, is still poorly understood. Here we examine the distribution of strain and magmatism in the portion of the TR making up the Nubia-Eurasia plate boundary. We use São Miguel Island because it stretches most of the TR width, which allows to investigate the TR's architecture and shedding light on TR's age and mode of deformation. From topography and structural analysis, and new measurements of 380 faults and dikes, we show that (1) São Miguel has two main structural directions, N150 and N110, mostly concentrated in the eastern part of the island as an onshore continuation of the faults observed offshore in the NE (N110 faults) and SW (N140) TR walls; (2) a new N50-N80 fault system is identified in São Miguel; (3) fault and dike geometries indicate that eastern São Miguel comprises the TR's northern boundary, and the lack of major faults in central and western São Miguel indicates that rifting is mostly concentrated at master faults bounding the TR. Based on TR's geometry, structural observations and plate kinematics, we estimate that the TR initiated between 1.4 and 2.7 Ma ago and that there is no appreciable seafloor spreading associated with rifting. Based on plate kinematics, on the new structural data, and on São Miguel's structural and volcanic trends, we propose that the eastern two thirds of São Miguel lie along a main TR-related transform fault striking N70-N80, which connects two widely separated N130-N150 TR-trending segments.

1. Introduction

Tectonic processes largely control the deformation in young, slow rifts like the TR, whereas asthenospheric processes greatly influence the evolution of mature mid-ocean ridges like the Mid-Atlantic Ridge (MAR) [e.g., *Magde et al.*, 1997; *Tucholke et al.*, 1997]. Most of our knowledge on the accommodation of the deformation during continental breakup comes from active continental rifts and passive margins [e.g., *Corti*, 2009; *Soares et al.*, 2012; *Bache et al.*, 2013], which show a zone of thinned crust, with or without formation of new oceanic crust [*Driscoll and Karner*, 1998; *Snow and Edmonds*, 2007]. The extensional plate boundaries have been classified from their structural, morphologic, and volcanic characteristics into two major types, mostly based on their spreading rate: "fast" (>60 mm/yr full rate) and "slow" (<60 mm/yr full rate). An intermediate type is often placed between them [e.g., *MacDonald*, 1982; *Francheteau and Ballard*, 1983; *Malinverno and Pockalny*, 1990].

The recognition of ultraslow rifts (<10 mm/yr full rate) is recent [e.g., *Michael et al.*, 2003; *Cannat et al.*, 2003]. Such rifts are characterized by a succession of magmatic and amagmatic segments that expose mantle peridotite directly on the seafloor [*Dick et al.*, 2003]. The mechanisms of deformation along the segments of ultraslow rifts are poorly understood when compared with the opening and deformation occurring along mature mid-oceanic ridges and continental rifts. This is mainly because (1) the ultraslow opening rates, which prevent the use of a classification based on their structural, morphologic, and volcanic characteristics, as used for the fast oceanic ridges; and (2) the morphology of ultraslow rifts is, more dominated by tectonics than by volcanism, which limits the use of gravity and magnetic anomalies [*Whittaker et al.*, 2008]. The knowledge of how deformation occurs along ultraslow rifts has only been deduced from seismic data [e.g., *Mutter and Karson*, 1992] and numerical modeling [e.g., *Van Wijk and Blackman*, 2005; *Henk*, 2006]. Several ultraslow rifts have been identified, for example, the Arctic Gakkel ridge [e.g., *Coalkey and Cochran*, 1998], the Southwest Indian Ridge [e.g., *Dick et al.*, 2003], and the Reykjanes ridges [e.g., *Appelgate and Shor*, 1994].

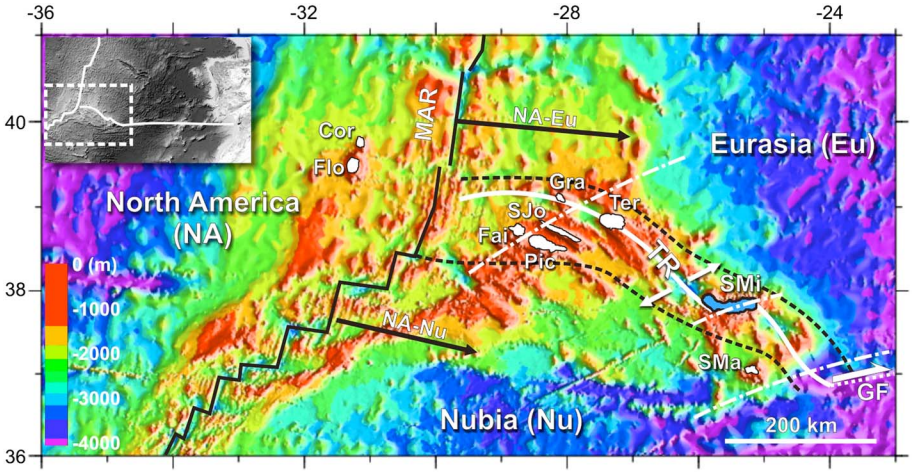

Figure 1. Bathymetric map of the Azores showing the tectonic setting in the Azores Triple Junction. Thick black lines indicate the location of the Mid Atlantic Rift (MAR) and associated transforms. Thick white line marks the axis of the Terceira Rift (TR). White dash-dotted lines mark the transform direction in the Azores resulting from counterclockwise rotation of Nubia (Nu) relative to Eurasia (Eu). Black dashed lines mark the diffuse Nu-Eu plate boundary (reproduced from *Marques et al.* [2013]). Black arrows represent velocity vectors of Eurasia (NA-Eu) and Nubia (NA-Nu) relative to fixed North America (NA) according to *DeMets et al.* [2010]. White arrows represent the relative motion between Eu and Nu [*DeMets et al.*, 2010], and extension in the TR close to São Miguel Island inset shows the location of the Azores archipelago in the Atlantic Ocean, with Iberia and NW Africa in the east. Bathymetry from *Lourenço et al.* [1998]. Islands: Cor, Corvo; Flo, Flores; Fai, Faial; Pic, Pico; SJo, São Jorge; Gra, Graciosa; Ter, Terceira; SMi, São Miguel; SMa, Santa Maria. GF, Gloria Fault with white half arrow indicating dextral strike slip. For the location of earthquakes, see Figure 2 in *Mendes et al.* [2013] and Figure 2 in *Marques et al.* [2013], and for the available focal mechanisms, see compilation in Figure 8 of *Borges et al.* [2007].

Here we focus on the early stages of rifting and on the deformation in the Terceira Rift (TR), an oceanic hyperslow rift [*Vogt and Jung*, 2004], along which the extension full rate is close to 4.5 mm/yr [e.g., *DeMets et al.*, 2010], therefore, about half the upper limit for ultraslow rifts. Since most of the TR lies below sea level, and the available geophysical data are scarce, we study the tectonic pattern of an island (São Miguel) that stretches most of the TR (Figure 1) to investigate the TR's behavior and evolution. The seismically and volcanically active TR is seemingly a young rift, and one of a few places in the world where the early stages of oceanic rifting can be investigated. We focus here on the TR's tectonics, volcanism, and age.

The TR comprises part of the boundary between the Eurasia and Nubia plates in the Azores region (Figure 1); therefore, the knowledge of its evolution is critical to the understanding of the evolution of the Azores Triple Junction (ATJ). In the TR's western half, the plate boundary is diffuse and therefore only part of the plate motion occurs within the TR [*Marques et al.*, 2013, 2014a; *Miranda et al.*, 2014]. In its eastern half, the TR takes up most of the deformation imposed by the relative motions between Nubia and Eurasia. The ATJ is currently diffuse, and it has been unstable over time with changes in both its position and configuration. Indeed, the old Eurasia/Nubia plate boundary is believed to have been the East Azores Fracture Zone (EAFZ) [e.g., *Laughton et al.*, 1972], and the migration from the EAFZ to the TR is considered to have occurred by successive jumps of short-lived rifts toward the NE [e.g., *Vogt and Jung*, 2004; *Sibrant et al.*, 2013a]. *Searle* [1980] proposed that the ATJ migration occurred during the rearrangement of plate poles, which induced the transfer of a wedge of European plate to the Nubian plate.

The Azores region shows also significant excess in magmatism and an abnormal shallow and thick plateau, the so-called Azores Plateau [*Searle*, 1976; *Detrick et al.*, 1995; *Gente et al.*, 2003; *Luís et al.*, 1998; *Silveira et al.*, 2010], which cannot be explained by the geometry and configuration of the ATJ alone [*Georgen and Sankar*, 2010]. The interaction with a mantle plume (hot or wet) below the Azores has thus been proposed as an explanation for the excess of volcanism in the region [*Vogt*, 1976; *Schilling*, 1985; *Thibauld et al.*, 1998; *Gente et al.*, 2003; *Métrich et al.*, 2014] and for the position of the Eurasia/Nubia rifting [*Vogt and Jung*, 2004]. Indeed, for some authors [*Cannat et al.*, 1999; *Gente et al.*, 2003] the plateau has formed by the eruption of underwater traps during the impact of a plume head of deep origin, around ~36 Ma and between 20 and 10 Ma, although tomographic data indicate shallow anomalies at the regional scale,

especially at the axis of the MAR [*Yang et al.*, 2006]. The geographic extension and the dynamics of the inferred mantle instability remain controversial. For several authors, the volcanism is not due to an active thermal mantle plume but rather reflects the existence of volatile-enriched upper mantle domains [*Schilling*, 1975; *Bonatti*, 1990; *Elliott et al.*, 2007] or wet spot [*Métrich et al.*, 2014]. Available geochronological data on the islands do not support a clear age progression along a well-individualized alignment, like in Hawaii or in Polynesia [*Morgan*, 1971; *Duncan and McDougall*, 1976; *Hildenbrand et al.*, 2004; *Ozawa et al.*, 2005]. Instead, isotope ages show synchronous volcanism during the last 1 Myr in the central and eastern Azores [e.g., *Hildenbrand et al.*, 2014; *Costa et al.*, 2014; *Sibrant et al.*, 2014], except on Santa Maria, which emerged around 5.7 Myr [*Sibrant et al.*, 2015a]. Furthermore, recent volcanic construction has resulted in the development of linear volcanic ridges elongated along two main directions: N150 and N110 [*Lourenço et al.*, 1998; *Hildenbrand et al.*, 2008a]. Such characteristics have been attributed to a significant control of volcanic outputs by regional lithospheric deformation [e.g., *Haase and Beier*, 2003; *Hildenbrand et al*., 2008a, 2014; *Marques et al*., 2013, 2014a], which is not in contradiction with a contribution from a mantle plume. Therefore, the formation of the TR can be due to plate tectonic or mantle plume origin.

The TR stretches from the MAR axis to the intersection with the EAFZ, as an approximately 620 km long sigmoidal graben, filled at regular spaces (approximately 80–100 km) by large-volume central-type volcanism building up islands and seamounts (Figure 1), which are from WNW to ESE: Graciosa Island [e.g., *Larrea et al.*, 2014; *Sibrant et al.*, 2014, 2015c], Terceira Island [e.g., *Casalbore et al.*, 2015; *Marques et al.*, 2015], the Dom João de Castro seamount, and São Miguel Island [*Zbyszewski*, 1961; *Moore*, 1990; *Forjaz*, 1993; *Johnson et al.*, 1998; *Forjaz et al.*, 2004; *Sibrant et al.*, 2015b]. The shape of the TR has been variably drawn as (mostly) continuous sigmoidal or segmented sigmoidal [e.g., *Vogt and Jung*, 2004] (present work). The continuous sigmoidal shape of the TR is a coarse representation of the bulk TR shape, which depends on an interpretation without local discontinuities, like transform faults. In contrast, here we suggest that the São Miguel transform has a segmented sigmoidal shape (Figure 1).

The Azores plateau displays quite a high level of seismicity [e.g., *Mendes et al.*, 2013, Figure 2; *Marques et al.*, 2013, Figure 2], but of low to intermediate magnitude (for the available focal mechanisms and magnitude, see compilation in Figure 8 of *Borges et al.* [2007]). The seismicity with $M_w > 4$ occurs mostly in the TR and along a graben-horst structure to the SW of the TR's western half [*Borges et al.*, 2007; *Marques et al.*, 2013]. Earthquakes in the Azores show a few characteristics that are remarkable: (1) it has been recognized since the early 1930s that very rare earthquakes (i.e., of tectonic origin and $M_L > 4$) have occurred inside the islands [e.g., *Agostinho*, 1931; *Machado*, 1959; *Borges et al.*, 2007]. Locally, low-magnitude earthquakes occur as swarms inside the islands, but they have been mostly attributed to volcanism rather than tectonics, which is the case, for the ongoing seismic crisis in São Miguel [*Silva et al.*, 2012a]. (2) From a total of 24 major earthquakes for which the focal mechanisms have been computed [*Borges et al.*, 2007], very few tectonic and $M_L > 4$ earthquakes are strike slip (4 out of 24), and by far, the large majority shows normal fault kinematics (16 out of 24) (*McKenzie* [1972], *Udías et al.* [1976], *Hirn et al.* [1980], *Moreira* [1985], *Grimison and Chen* [1986], *Buforn et al.* [1988], *Miranda et al.* [1998], *Buforn et al.* [2004], and *Borges et al.* [2007] for a synthesis). (3) The main fault trends associated with tectonic $M_L > 4$ earthquakes are the WNW-ESE (approximately N110-N120) and NNW-SSE trends (approximately N140-N150). (4) *Marques et al.* [2014b] proposed, based on the 1998 Faial earthquake and previous earthquakes in the Azores with similar fault plane solutions, that the ENE-WSW fault system is critical to the understanding of geodynamics in the Azores, because it is coincident with the TR-related transform direction.

Previous studies have suggested that rifting in the TR started circa 45 Myr ago [*Krause and Watkins*, 1970], circa 36 Myr ago [*Searle*, 1980], less than 5 Myr ago [*Luís et al.*, 1998], less than 1 Myr ago [*Vogt and Jung*, 2004], or during the last 25 Myr [*Luís and Miranda*, 2008]. Considering the oldest proposed TR age (i.e., 45 Ma) and an average opening rate of approximately 4.5 mm/yr reported for the Nubia/Eurasia plate boundary in the Azores [*DeMets et al.*, 2010; *Marques et al.*, 2013], then the TR would have already opened approximately 203 km (45 Ma × 4.5 mm/yr), which appears rather implausible given the current narrow geometry of the TR. Recognizing that the oldest ages (>5 Myr) are not consistent with the estimated opening in the TR, *Sibrant et al.* [2015a] suggested from new geochronological data on Santa Maria Island that the easternmost part of the TR initiated less than 2.8 Myr ago. The creation of new oceanic crust in the TR has never been unambiguously shown, likely because hyperslow rifting makes the recognition of magnetic anomalies difficult [e.g., *Krause and Watkins*, 1970; *Searle*, 1980]. This supports a more recent initiation of the TR, in agreement with recent studies [*Vogt and Jung*, 2004; *Sibrant et al.*, 2015a]. Here we estimate the age of the TR and analyze if there has been spreading and the creation of new oceanic crust within the TR.

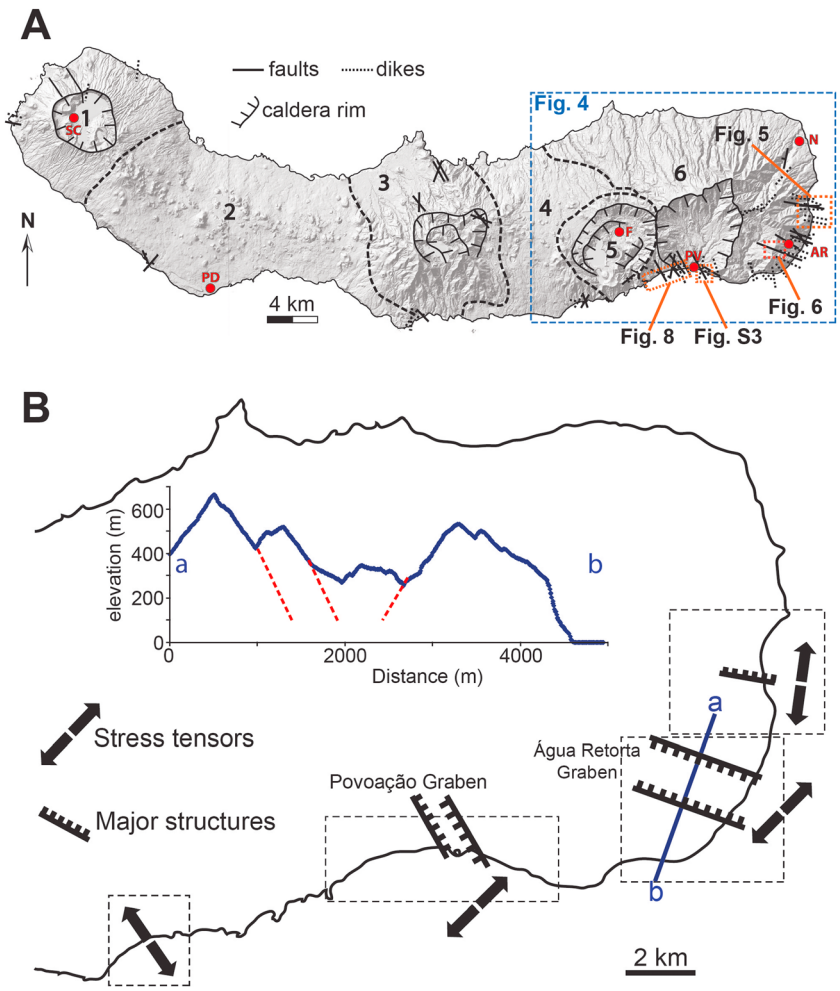

Figure 2. (a) Shaded relief map of São Miguel generated from a high-resolution DEM (10 m) showing the main volcanic complexes (delimited by black dashed lines) as defined by *Moore* [1990]: (1) Sete Cidades volcano, (2) western fissural system, (3) Fogo volcano, (4) eastern fissural system, (5) Furnas volcano, and (6) Nordeste complex. Solid and dotted black lines summarize and localize our measurements of faults and dikes, respectively. Solid black lines with ticks mark the position of inferred calderas reported in previous work. Red circles indicate main cities/villages: Sete Cidades (SC), Ponta Delgada (PD), Furnas (F), Povoação (PV), Água Retorta (AR), and Nordeste (N). A clean version of the shaded relief map of São Miguel is given as Figure S1 in the supporting information. (b) Location of the main structures recognized in eastern São Miguel. Dashed rectangles show the location of the four zones distinguished here. Black arrows indicate the stress tensors of the four zones, deduced from the orientations of the principal stress axes shown in Figure 4. Line a-b marks the location of the NNE-SSW topographic profile of the Água Retorta graben shown in the inset. Red dashed lines represent the main faults defining the graben.

We focused our attention on the tectonics of São Miguel Island, because the eastern part of São Miguel has grown on the northern shoulder of the TR, and the central and western parts have grown inside the TR. The unique position of São Miguel inside the TR allows the observation and measurement of tectonic and volcanic elements, which can be linked to the architecture and evolution of the TR in its eastern half, where the Nubia/Eurasia plate boundary seems currently discrete. From onshore and offshore available morphologic and geophysical data, combined with structural analyses and the measurement of more than 380 faults and dikes, we discuss the relationships between tectonics, volcanism, and the TR's age and shape.

2. Geological Background

São Miguel is the largest island of the Azores Archipelago (Figure 1) and has developed in the SE part of the TR. On the most recently available geological map [*Moore*, 1990, 1991], six volcanic complexes (VC) have been distinguished (Figure 2), which are from west to east: (1) the Sete Cidades VC, (2) a western fissural VC mostly

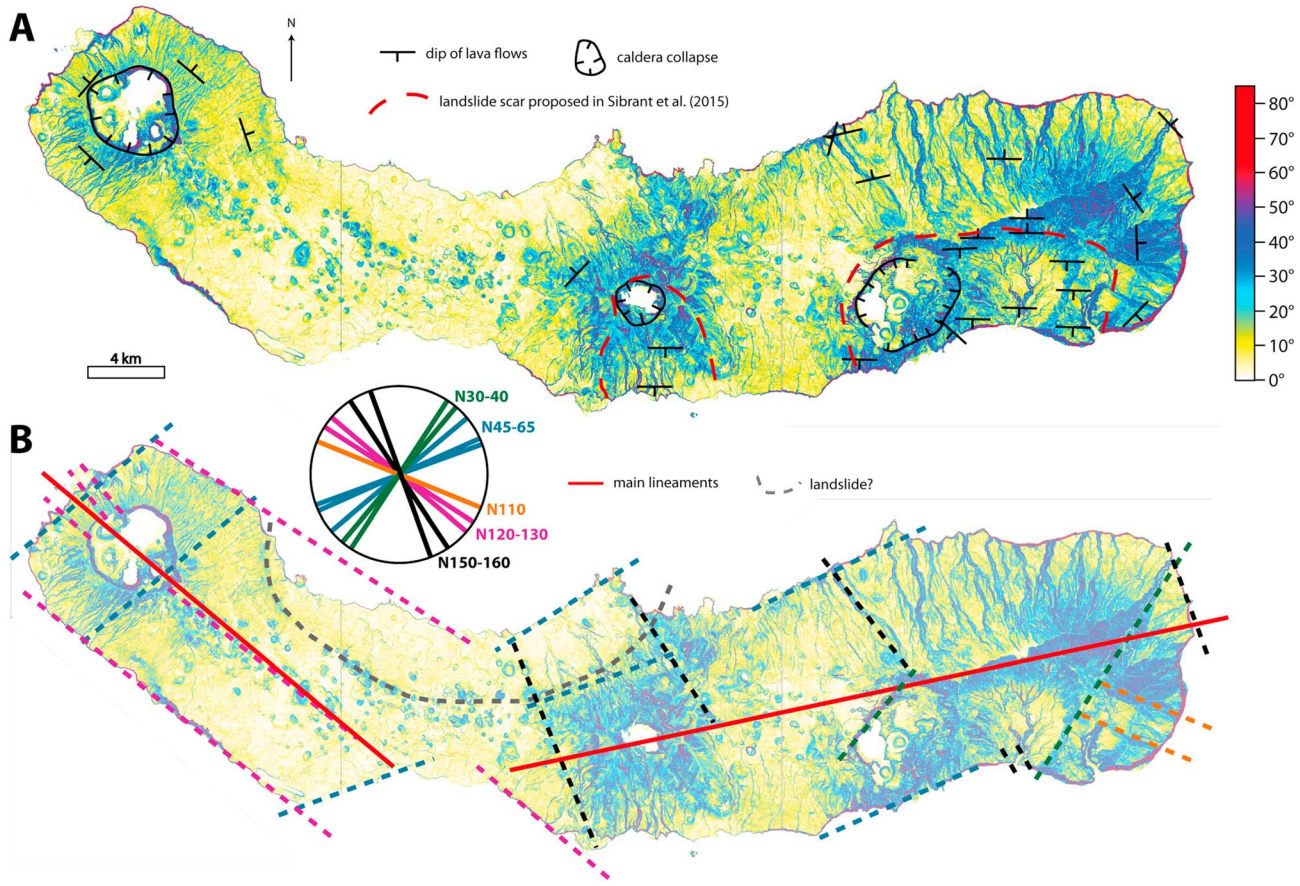

Figure 3. (a) Slope map of São Miguel generated from the high-resolution digital elevation model (DEM) with indication of dip of lava flows measured during our fieldwork. (b) Our interpretation of major lineaments. The color code indicates the direction of the interpreted lineaments.

made of aligned strombolian cones, (3) the Fogo VC, (4) a eastern fissural VC, (5) the Furnas VC, and (6) the Nordeste VC. *Forjaz* [1997] provides a review on the volcanism of São Miguel. Recent geochronological data acquired on the various VCs show that the subaerial volcanic construction of São Miguel occurred during the last 1 Myr [*Moore*, 1990; *Moore and Rubin*, 1991; *Johnson et al.*, 1998; *Sibrant et al.*, 2015b].

The major central volcanic edifices of São Miguel have been affected by one or more collapse events (Figure 2). *Zbyszewski et al.* [1959, 1961] concluded that the Sete Cidades volcano (Figure 2) was affected by one caldera collapse, while for *Queiroz et al.* [2008] the collapse has occurred in three stages. The Sete Cidades volcano comprises a graben in its northwestern flank [*Machado*, 1959]. The Fogo volcano (Figure 2) has been affected by one or two caldera collapses [*Zbyszewski et al.*, 1959; *Zbyszewski*, 1961; *Moore*, 1990] and presents active volcanic structures with a N150 trend, which could possibly make up a graben-hosting hydrothermal systems [*Carvalho et al.*, 2006]. The Furnas volcano (Figure 2) has been affected by at least one caldera collapse event [e.g., *Moore*, 1990; *Duncan et al.*, 1999]. The Nordeste VC (Figure 2) exhibits a circular depression, concave toward the south, referred to as the Povoação caldera [*Moore*, 1990]. More recently, *Sibrant et al.* [2015b] proposed that arcuate morphological scars in both eastern and central São Miguel have been created by large lateral flank collapses (Figure 2). In SE São Miguel, especially, the Povoçao depression partly results from a large catastrophic landslide that removed the whole southern flank of Nordeste volcano between 750 kyr and 500 kyr ago [*Sibrant et al.*, 2015b]. An additional landslide scar was also proposed for the southern flank of Fogo volcano.

Two main structural trends have been identified in São Miguel, the N110 and N150, which have apparently controlled the position and distribution of the volcanic edifices [*Zbyszewski et al.*, 1959, 1961; *Moore*, 1990; *Forjaz*, 1993]. The geological map of *Moore* [1990] indicates several normal faults, but it does not show the main dike swarms. Some dyke trends were reported earlier in the map of *Zbyszewski et al.* [1959], but their meaning deformation within the context of the TR has not been addressed and discussed.

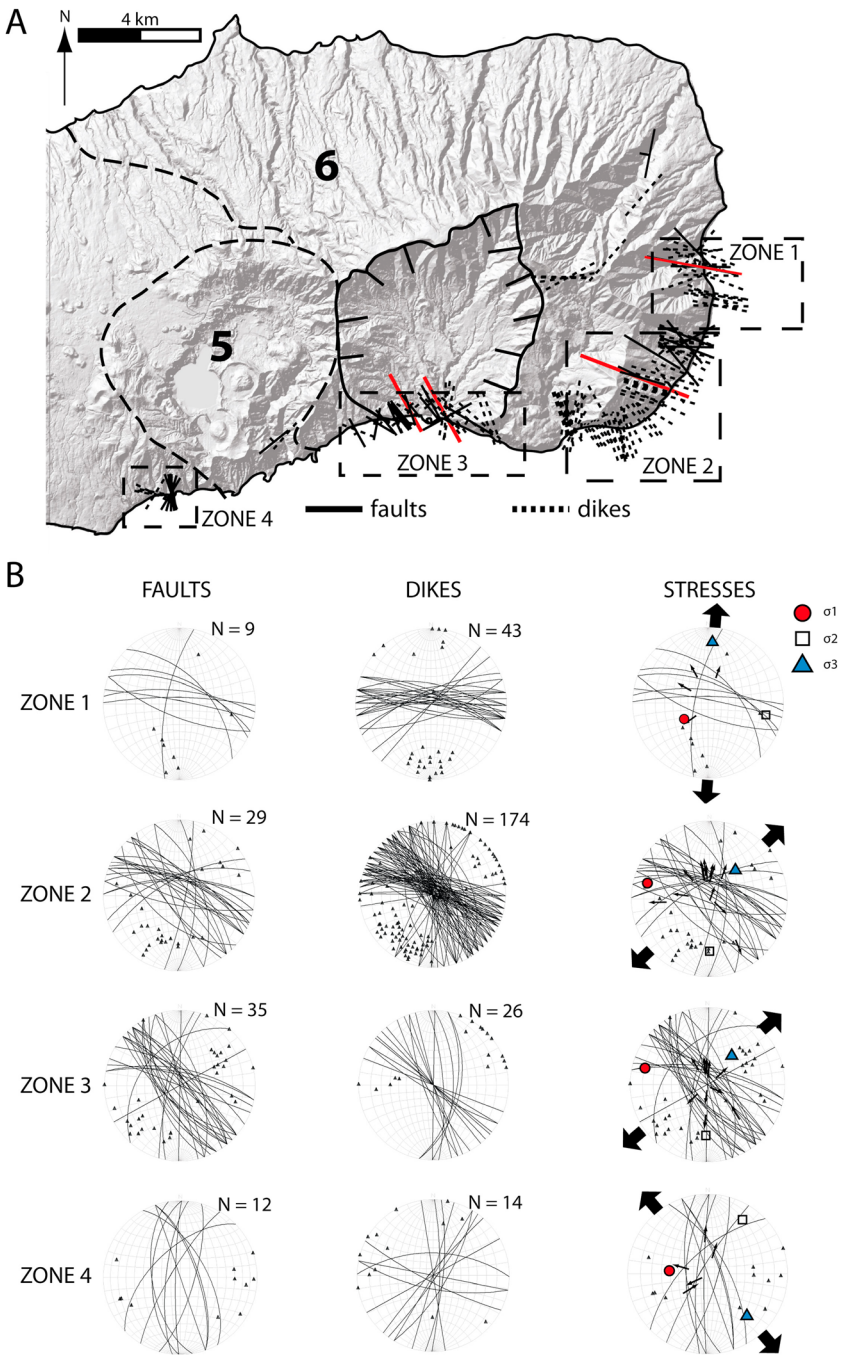

Figure 4. (a) Shaded relief map with the measured faults and dikes for the eastern part of São Miguel. Dashed squares indicate the four zones distinguished from our new morphological analysis, fieldwork observations, and tectonic markers. Fault and dike locations are simplified for clarity. Red lines indicate the main structures recognized in this study. (b) Computation of great circles and poles to planes (Wülff net, equal angle lower hemisphere projection) of the faults, dikes, and stress tensors for zones 1–4. *N* is the number of measurements. Red circle = σ_1; square = σ_2; triangle = σ_3.

3. Methods

3.1. Morphostructural Analysis and Fieldwork

The overall morphology of São Miguel is dominated by two main trends: a N80 trend in the eastern two thirds of the island and a N130 trend in the western one thirds of the island (Figure 2). In order to define the main topographic lineaments within the island and identify zones of potential major interest for fieldwork and

Table 1. Results of the *P-T* Method, NDA, and Inverse Method

		PBT			NDA				Inverse				
Site	*N*	*P*	*B*	*T*	$\lambda 1$	$\lambda 2$	$\lambda 3$	Strain Ratio	$\sigma 1$	$\sigma 2$	$\sigma 3$	Stress Ratio	Method Used
Zone 1	4	270/79	83/28	211/06	294/84	113/06	203/00	0,2875	237/59	102/23	3/20	0,132	INV
Zone 2	13	257/79	105/24	01/02	262/78	102/12	11/04	0,3784	285/21	180/34	40/48	0,679	INV
Zone 4	10	138/87	309/04	36/02	239/88	124/01	33/02	0,5544	249/72	125/10	32/14	0,901	INV
Zone 5	5	284/73	180/02	89/07	300/76	171/09	79/11	0,224	274/51	33/21	137/31	0,131	INV

structural analysis, we combined the information from the map of *Zbyszewski et al.* [1959], a digital elevation model (DEM) of the island at a spatial resolution of 10 m, and a slope map built from the DEM (Figures 2–4 and S1 in the supporting information). By varying the illumination angles, we could detect the main directions previously recognized (N150, N110). The slope map was used to detect topographic patterns (mostly major lineaments and slope breaks) without the bias of the illumination angle. Then we used topographic profiles to recognize and characterize areas potentially affected by major tectonic structures such as grabens and collapse scarps.

Fieldwork was then focused on the recognized lineaments to characterize and measure fault elements and dikes throughout the island. The outcrops are mainly localized along the coastal cliffs and canyons in the island, which constitute natural sections and represent by far the great majority of the outcrops on the island. We systematically measured the geometry (strike and dip) of dikes and faults and defined their kinematics from available markers (striations, shear criteria, and offset). A total of 104 faults and 276 dikes were measured in the whole island.

3.2. Data Processing

All the measured strikes were corrected for the present magnetic declination (www.rncan.gc.ca). Fault and dike data were processed using the tectonics software FP v1.7.5 [*Ortner et al.*, 2002] for the determination of the orientations of the principal stress axes. Only fault data with observed striations were used to calculate the orientations of the principal stress axes.

Principal strain axes were calculated using the *P-T* method [*Turner*, 1953], the direct inversion method [*Angelier*, 1984; *Angelier*, 1994], and the numerical dynamic analysis [*Spang*, 1972]. The *P-T* method calculates the *P* axis (shortening axis), *B* axis (intermediate principal strain axis), and *T* axis (extension axis) for each fault plane and generates mean axes for a given fault set. The direct inversion method is based on the assumption that the direction and sense of slip on a single fault plane are those of the shear stress called maximum. The resolved shear stress is applied on this plane by the stress tensor [*Wallace*, 1951]. The commonly used stress inversion technique results in the orientation (azimuth and plunge) of the principal stress axes of a stress tensor: the stress ratio $R = (\sigma_1 - \sigma_2)/(\sigma_1 - \sigma_3)$ describes the relative stress magnitudes. The principal stress axes σ_1, σ_2, and σ_3 are the maximum, intermediate, and minimum stress axes, respectively. The inversion method aims at determining the stress tensor that best accounts for the strikes and sense of movement in massive rock indicated by a lineation. It fails in the analysis of strongly asymmetric fault sets, e.g., when one set of conjugate faults dominates over the other [*Sperner et al.*, 1993]. The numerical dynamic analysis (NDA) allows the determination of the reciprocal strain tensor ($\lambda_1 \geq \lambda_2 \geq \lambda_3$) and strain ratio, $R_{\text{strain}} = (\lambda_2 - \lambda_3)/(\lambda_1 - \lambda_3)$. For all analyses, the angle (θ) between λ_1 and λ_2 was assumed to be 30°, which is a reasonable value for the angle of internal friction of newly formed faults [*Byerlee*, 1967], and is an average angle for fault sets consisting of preexisting faults [*Sperner and Zweigel*, 2010].

In order to determine the different populations of faults in the various sectors of the island (zones), we used the *P-T* axis method. The method chosen for a given fault population was based on the best fit of principal axes orientations with respect to fault strike and dip. Our results suggest that the principal axes of most of the brittle fault sets are best represented by the inverse method (Table 1), and the resulting stress tensors are shown in Figure 4.

4. Results

4.1. Morphology

The slope map, combined with the shaded relief map, reveals major lineaments in São Miguel (Figures 2 and 3). The overall shape of the island indicates two main lineaments (red lines in Figure 3b): N130 in the west and N80

in the east. These lineaments are also present along the current straight coastal lines of the island (Figure 3b). Onshore, the alignment of scoria cones in the west define a N130 trend, ESE of Sete Cidades, and a N150 trend on the ENE and WSW flanks of the Fogo volcano. This trend can be also observed in the canyon to the north of Furnas and inside the depression of Povoação. On the NE end of the island, a major canyon deeply incises the Nordeste volcano along a N30 azimuth. A similar trend is observed on the straight northwestern wall of the Furnas caldera. Two linear scarps can be recognized on both sides of Água Retorta village (Figures 2 and 3). Finally, on the northern flank of the western third of the island, and also part of the transition to eastern São Miguel, a major curved scarp can be observed, marked by both topographic slope breaks and curved alignments of young scoria cones. The slope map reveals also that Sete Cidades is a well-preserved volcano with irregular coastal line, radial canyons, and external slopes comprised between 5 and 20° (Figure 3). The summit of the volcano shows a large elliptical caldera. The NW part of Sete Cidades comprises a graben structure trending N130, compatible with the elongated western part of the island [*Moore*, 1990]. SE of Sete Cidades the slope decreases to values below 5°, which indicates that we are probably out of the Sete Cidades domain. The eastern part is covered by several well-preserved strombolian cones aligned along N130 (Figures 2 and 3). The tectonic and volcanic lineaments are parallel to the local elongated trend of the island and to the TR and do not show a radial pattern around the central edifice of Sete Cidades. This suggests that the tectonic and volcanic trends are likely primarily controlled by a regional stress field, rather than an isotropic stress field due to the hydrostatic effects of a central magma chamber [e.g., *Nakamura et al.*, 1977] or the stress field resulting from the load of the Sete Cidades volcano (which could produce a radial pattern of dykes [e.g., *Roman and Jaupart*, 2014]). East of the strombolian cones (domain 2), the general trend of the island changes from approximately N130 to approximately N80 and comprises, from west to east, the volcanoes of Fogo, Furnas, and Nordeste.

The analysis of the shaded relief and slope map reveals also an asymmetric morphology of the eastern part of the island (domains 3–6): the northern flank of the island is quite regular and characterized by gentle external slopes ($<$25°, excluding the slopes inside canyons), while the southern side is much more irregular (Figure 3). It comprises several structures, e.g., a subcircular caldera, a series of canyons, and coastal cliffs of various heights. The elongated N80 part of the island has been also affected by several flank collapses toward the south as recognized by *Sibrant et al.* [2013b, 2015b]. The transition between domain 2 and the Fogo volcano is marked by a variation of the nature of the volcanism (small strombolian cones versus large central volcano), as the slope increases from 5° to more than 20°, and by the presence of numerous canyons that deeply incise the flanks of Fogo volcano. The external slopes of Fogo seem much more incised by canyons than the other main volcanoes and show a trend close to N-S in the southern sector (Figures 2 and 3). To the east, domain 4 shows gentle slopes and is relatively poor in deep canyons. As in domain 2, it shows several strombolian cones, but aligned along a N80 trend, so again parallel to the local elongation of the island. The easternmost part of the island comprises domains 5 and 6 and shows much sharper and deeper canyons, with the main canyon trending ~N50, irregular topography and abrupt slope variations. The northern part shows a relatively regular slope incised by deep canyons. The southern part shows two elliptical structures, which have been identified as the Furnas and Povoação calderas. On the southeastern end of the island, we can identify two scarps with approximately N110-N120 trend, which can be interpreted as a graben structure. The entire eastern sector of the island seems affected both by erosion (without particular orientation) and by linear structures with a potential tectonic origin.

4.2. Tectonics

The eastern end of São Miguel is cut by faults and dikes almost exclusively striking N110. We designate this sector of the island Zone 1 (Figure 4). The stress tensor in Zone 1 indicates an approximate N-S trending σ_3 axis and a subvertical σ_1, which is consistent with the mean E-W strike of dikes measured in the eastern part of the Nordeste VC. In this sector dykes and faults affected rocks dated between 880 and 750 ka by *Johnson et al.* [1998] and *Sibrant et al.* [2015b], which provides a maximum age of 750 ka for deformation. The related stress state is recorded only in the easternmost part of the Nordeste VC. In Zones 1 and 3, several faults oriented N110 and dipping to the NNE show an apparent normal offset up to 20 m. The outcrop in Figure 5 comprises a normal fault striking N110 and shows a displacement larger than the height of the outcrop.

Immediately to the south of Zone 1, in Zone 2, two linear scarps oriented N110 can be identified on both sides of Água Retorta (see also Figure 2). Rocks dated at circa 750 ka [*Sibrant et al.*, 2015b] bound a broad and linear topographic depression, which reaches a length of about 4 km and a width of 2.5 km inland (Figures 3, 4, and S1

Figure 5. Image showing main normal fault dipping to the north in the eastern end of the island. Location of the outcrop is shown in Figure 2.

in the supporting information). There, faults and dikes strike either N110 or N150 (Figure 4). Zone 2 also comprises a set of major faults oriented N115, dipping from 60 to 65° to the NE (Figure S2 in the supporting information). The most significant shows a minimum offset of 25 m. The fault plane presents striations with a measured pitch of 80° toward the east. These faults correspond to the southern scarp bounding the N110 depression. The topographic profile (Figure 2b) indicates that the Água Retorta depression is probably a graben structure. Although a northern scarp is visible on the DEM (Figures 4 and S1 in the supporting information), no faults or dikes could be observed due to dense vegetation. Thus, topographic evidence, orientation, dip, and kinematics of the faults and deduced stresses (Figures 4 and 6) suggest that the depression consists of a graben made up of several faults striking N110 and dipping to NE and SW, but we did not find full evidence for a graben, so we keep in mind that it could be a half-graben. The southern scarp shows a minimum vertical height of nearly 250 m. The graben is asymmetric and contains at least two small volcanic cones.

Immediately to the west of Zone 2, Zone 3 coincides with the southern part of the Povoação depression (Nordeste VC, Figure 2), which is characterized by faults and dikes mostly striking N150 (Figure 4). The stress tensors for Zones 2 and 3 indicate approximate NE-SW extension, which is observed in two of the four zones defined in the present work. Both zones are located in the Nordeste VC (Figures 2 and 4). To the west of the city of Povoação (Zone 3, Figure 2), the coastal cliff shows a major tectonic discontinuity (Figures 7 and S3 in the supporting information), which separates a southwestern succession of numerous lava flows dipping

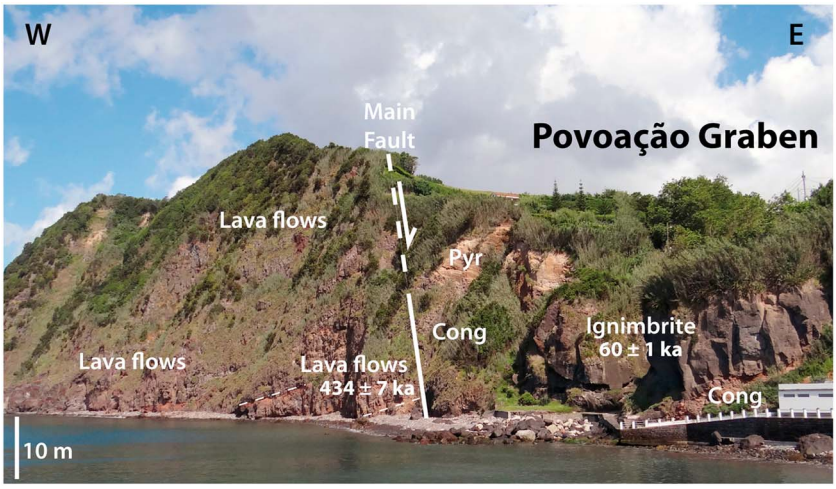

Figure 6. Image of the E-W sea cliff to the west of the village of Povoação (see Figure 2 for location and supporting information Figure S3 for a unannotated version of the picture). The white full line marks the observed and measured main fault defining the western wall of the Povoação Graben and separating an older stack of lava flows (dip marked by white dotted lines) from a much younger succession of conglomerates (Cong), ignimbrite, and mixed pyroclasts and cinders (Pyr). The inferred prolongation of the fault in the upper half of the cliff is marked by a white dashed line. The thinner white dashed lines indicate the dip of lava flow. The K-Ar ages refer to samples SM12AJ and SM12E in *Sibrant et al.* [2015b]. Minor normal faults can be recognized on the image but are not marked for the sake of clarity.

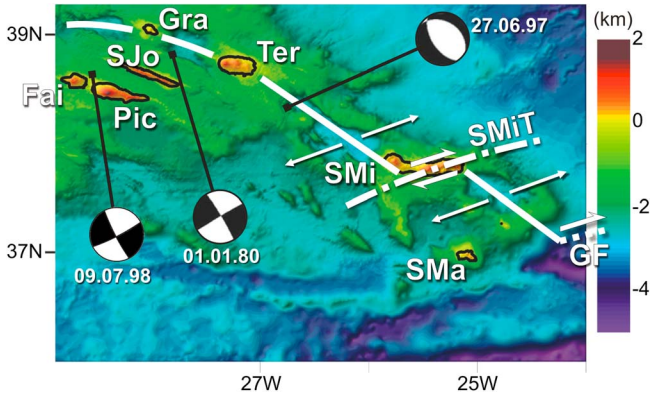

Figure 7. Schematic interpretation based on plate kinematics and new structural observations, mostly the newly recognized N70-N80 fault system. The proposed São Miguel transform fault (dash-dotted white line denoted SMiT) separates two segments of the Terceira Rift, the Hirondelle Basin in the NW and the Povoação Basin in the SE, and should be dextral strike slip (indicated by the white half-arrows, and similar to the Gloria Fault = GF) as the result of opening in the N80 direction (as indicated by plate kinematics and represented by the white arrows). Fault plane solutions for three earthquakes in the Azores (09.07.98 from *Marques et al.* [2014b] and the other 2 from *Borges et al.* [2007]) are relevant for the present study. Thick white line represents the Terceira Rift. Islands: Fai, Faial; Pic, Pico; SJo, São Jorge; Gra, Graciosa; Ter, Terceira; SMi, São Miguel; SMa, Santa Maria.

gently to the SW, from a northeastern succession of conglomerates, ignimbrite flow comprising fiamme at the base, and mixed pyroclasts and cinders. These two successions are separated by a major fault striking N140 and dipping 70° to the east (Figures 7 and S3 in the supporting information). To the east of Povoação, we also identified normal faults striking N150 and dipping between 70° and 80° to the WSW and ENE (Figure S4 in the supporting information). The faults bound a depressed block approximately 1 km long, which has been apparently downthrown by a minimum of 125 m. The stress tensor estimation for Zone 3 (Figure 4b) and stereoplots both indicate the presence of a graben, here coined the "Povoação Graben" (Figure 6). *Sibrant et al.* [2015b] reported an age of 434 ka for the rocks cut by this graben.

Finally, Zone 4 is located to the SW of the Furnas volcano, where faults and dikes strike N-S and N20-N50. The stress tensor in Zone 4 indicates σ_3 with a NW-SE direction and subvertical σ_1. This stress regime is recorded throughout the Furnas Complex and is different from the stress tensor obtained for the other three zones. This stress state is only recorded in rocks dated younger than 93 ± 9 ka by *McKee and Moore* [1992].

Most of the measured faults exhibit a dominant normal component, with individual offset commonly less than 1 m. In total, more than 94% of the recognized structures are located in the eastern part of the island. In the NW part of Sete Cidades we measured the southern wall of the graben (N160) identified by *Moore* [1990]. A major fault, in the NW, strikes N110 and dips 65° to the SSW, and two other faults strike N50 and dip 80° to the SE. At the base of the Fogo volcano (Figure 2), we measured faults and dikes striking N150 and N50.

5. Discussion

Plate kinematics [e.g., *McKenzie*, 1970, 1972; *Laughton and Whitmarsh*, 1974; *Argus et al.*, 1989; *DeMets et al.*, 1990; *Kiratzi and Papazachos*, 1995; *Calais et al.*, 2003; *Serpelloni et al.*, 2007; *DeMets et al.*, 2010] and thin sheet modeling [e.g., *Jiménez-Munt and Negredo*, 2003] indicate extension along N70-N80 in the São Miguel sector of the TR. In contrast, seismicity and GPS have indicated different trends for extension in the same area. From seismicity, *Borges et al.* [2007] estimated maximum extension along approximately N45 (in contrast to the N70-N80 from plate kinematics), and *Bezzeghoud et al.* [2014] found even greater discrepancies between extension determined from seismicity and plate kinematics. *Bezzeghoud et al.* [2014] justified the discrepancies in extension trend between seismicity and plate kinematics with the change over time between the dominant forces born in the plate and in the underlying mantle (the latter justifying the current discrepancies). We add that the discrepancies could be due to the very short time of seismic observation, which can be strongly affected by strain partitioning on the studied faults. For instance, two earthquakes in the TR (Figure 7) show fault plane solutions with similar strike but contrasting kinematics: pure sinistral strike slip for the 01.01.80 shock [*Hirn et al.*, 1980] and pure normal fault for the 27.06.97 shock [*Borges et al.*, 2007]. Using GPS data obtained within São Miguel Island in two campaigns (2000 and 2002), *Trota et al.* [2006] concluded that São Miguel accommodates moderate N121 extension, in great contrast to the approximately N80 extension estimated from plate kinematics [see also *Fernandes et al.*, 2003, 2004, 2006]. This discrepancy was recognized by *Trota et al.* [2006], but the authors did not propose any explanation. Our interpretation is that

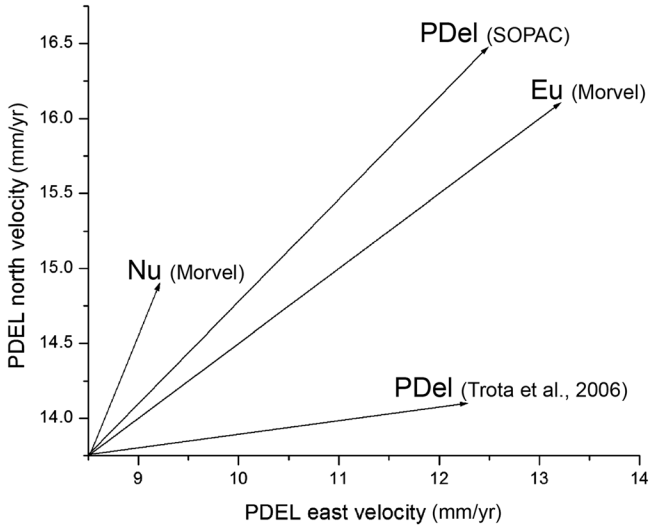

Figure 8. Plot showing the comparison between PDel velocities according to *Trota et al.* [2006] and SOPAC (2015) and between PDel (SOPAC) and Morvel Nubia (Nu) and Eurasia (Eu) velocities. Note that currently, the PDel velocity is closer to Eurasia velocity according to the Morvel plate velocity model.

the discrepancy could be due to (1) a short time period of GPS survey (2000–2002), (2) an extremely short time period of observation in each station (2.5–3.0 h), (3) a very large error (e.g., 12 mm repeatability), and (4) GPS stations located on the slopes of two major volcanoes mostly made of unconsolidated and unstable pumice, which results in a large scatter in the values of the ground motion, including opposite directions [cf. *Trota et al.*, 2006, Table 3 and Figure 6], most likely due to significant local soil creeping.

Regarding absolute ground motion in São Miguel, *Trota et al.* [2006] concluded that a mean velocity vector for the period 1993–2002 at site PDel (Ponta Delgada) fits approximately the velocity of the Nubia plate, as given by the REVEL model. Meanwhile, calculations using SOPAC (sopac.ucsd.edu/velocities.shtml using IGS08 reference frame) for August 2015 and the same permanent station in Ponta Delgada (site PDel) give a north velocity $V_n = 16.5 \pm 0.1$ mm/yr and an east velocity $V_e = 12.5 \pm 0.2$ mm/yr. The new value for V_n is greater by 2.4 mm/yr when compared with the value given by *Trota et al.* [2006] for the same site (PDel in their Table 4)(Figure 8). Calculations using Morvel (geoscience.wisc.edu/~chuck/MORVEL/motionframe_nnrm56.html) give the following values (Figure 8): Eurasia: $V_n = 16.1$ mm/yr, $V_e = 13.2$ mm/yr, Az = N39.2; Nubia: $V_n = 14.9$ mm/yr; $V_e = 9.2$ mm/yr, Az = N31.7. Plotting all these velocities we obtain the graph presented in Figure 8, which shows that this part of São Miguel Island is moving at a velocity closer to that of Eurasia. The velocity vector for site PDel trends approximately N37, which is similar to the trend obtained by GPS for Terceira Island [*Marques et al.*, 2015], also inside the TR but farther NW.

Seismicity within São Miguel is mostly characterized by swarms of low-magnitude earthquakes. *Silva et al.* [2012a] filtered 15,000 shocks recorded between 2002 and 2010 and used the 78 best located events to compute fault plane solutions, which were inverted for the best fitting stress tensor. *Silva et al.* [2012a] concluded that the seismic swarms are volcanic in origin, with a possible tectonic control. They also concluded that the stress tensor varies in space (both horizontally and vertically) and time. Using all the 78 fault plane solutions, they concluded for a stress field with subhorizontal σ_1 striking WNW-ESE and σ_3 striking NNE-SSW, similar to the stress field using only the fault plane solutions located in the Fogo area. For the Congro area (neighboring Fogo to the east), the stress field shows subhorizontal σ_3 striking NNE-SSW and near-vertical σ_1. The stress field below 5 km shows a switch between σ_1 (subhorizontal) and σ_3 (subvertical). Given the kinematics reported in *DeMets et al.* [2010], and the fact that São Miguel lies inside the TR, one would expect σ_3 striking approximately N70 and σ_1 subvertical. This would be in agreement with the fault plane solution of the 1989 major earthquake that occurred to the NW of São Miguel [*Borges et al.*, 2007]. However, four critical factors must be taken into account when analyzing the stress field responsible for the tectonic structures observed inside the island: (1) the volcanic ridge has its own internal stress field, which greatly depends on topography; (2) the load of the whole volcanic ridge on the underlying crust distorts the regional stress field; (3) the fluids (gas and liquid water, and magma) related to active volcanism may greatly control the local stress field due to fluid overpressure and magma pressure; and (4) most of São Miguel lies on the intersection between two main fault systems, the N130 (normal faults) and the N80 (strike-slip faults). Therefore, fault plane solutions computed from earthquakes that occurred inside the volcanic ridge or below it reflect the sum of the effects of all those factors, although locally some factors may be more important than others.

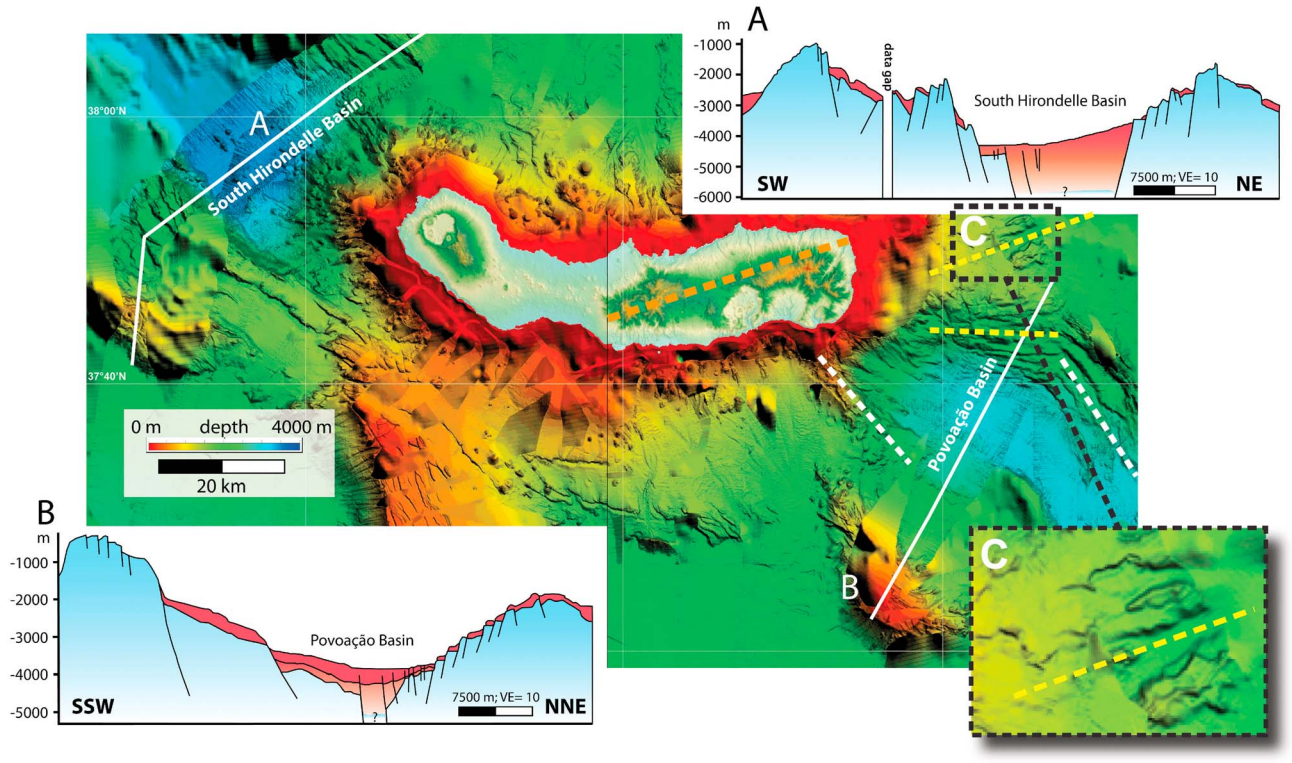

Figure 9. Bathymetry around São Miguel showing the South Hirondelle and Povoação Basins located NW and SE of the island, respectively. The basins are bounded by linear scarps coinciding with the master faults of the TR. White lines (A and B) indicate the location of the seismic profiles shown in insets A and B (both from *Weiß et al.* [2015a]). VE = vertical exaggeration. Question marks indicate the uncertain location of the sediment/basement interface. Inset C shows zoom of the region east of São Miguel Island marked by dashed black rectangle, where N70-N80 fault scarps can be recognized offshore (dashed yellow line), which is parallel to the trend of the eastern two thirds of São Miguel Island (marked by dashed orange line). Dashed white lines represent the N140-N160 fault system in the Povoação Basin SE of São Miguel, which stretches into the island as the N150 fault system we measured in the present study.

Zandomeneghi et al. [2008] used tomographic inversion of local earthquake arrival times (*P* and *S* phases from 289 earthquakes recorded by a network of 20 seismometers) to model the crust in the shallowest 5–6 km. They found two contrasting directions of low (NW-SE) and high (NE-SW) seismic velocities and interpreted them as the effects of pyroclastic deposits, intrusive bodies, geothermal fields, and tectonics.

Although on a much smaller scale (a 15 km^2 area on the NNW slope of Fogo volcano), *Gandino et al.* [1985] recognized the presence of the ENE-WSW fault system from a geophysical survey to a depth of more than 1 km, which means that the N70-N80 fault system exists inside the island. In the same geophysical survey, *Gandino et al.* [1985] also detected the N130-N150 fault system, which can be recognized offshore SE of São Miguel on the bathymetric chart shown in Figure 9 (SW shoulder of the TR offshore SE of São Miguel).

Based on the available information, we note that the geophysically detected trends are similar to the main fault directions we measured at the surface in the present study, which means that they likely have a deep expression and affect the whole edifice and part of the underlying crust.

5.1. Tectonic Control on the Development of São Miguel

Given that erosion is a secondary factor because of the recent age of most volcanism (except in easternmost São Miguel), the shape of São Miguel, and the various morphologic and tectonic markers (alignment of main volcanic edifices and scoriae cones and trends of faults and dykes) suggest that they result dominantly from its volcano-tectonic evolution, i.e., that regional plate motions exert a strong control of deformation on the architecture and evolution of the island. The N80 alignment of three major volcanoes (Nordeste, Furnas, and Fogo) in the eastern two thirds of São Miguel (Figure 3) is a conspicuous feature, whose geodynamic meaning has not been discussed in earlier studies. The N80 trend not only suggests a structural control on the major volcanic outputs but also has important imprint on the development of erosion and mass wasting

[*Sibrant et al.*, 2015b]. Indeed, the N80 orientation bounds contrasted sectors comprising regular constructional slopes in the northern part and several morphostructural depressions affecting the southern part. Such asymmetry is unlikely to result solely from differential coastal erosion, as dominant tide and marine wave impact dominantly occurs in the northern sector, which appears the less affected. Although we have not directly observed and measured N80 faults, we note that (1) several coastal segments and volcanic lineaments also show a linear aspect roughly elongated along a ENE-WSW direction (Figure 3). Such linear coastlines depart from the typical concave shape of coastlines developed on major volcanic edifices. (2) *Gandino et al.* [1985] found the ENE-WSW fault system on the northern slope of Fogo volcano, thus attesting to its existence at depth, although not directly observed at the surface. (3) The N70-N80 fault system can also be recognized offshore the eastern end of São Miguel in the bathymetric chart shown in Figure 9. The meaning and possible kinematics of the ENE-WSW trend may thus have a regional geodynamic significance, which is further discussed in section 5.3.

The western part of São Miguel is clearly elongated along the N130 direction and is also bounded by conspicuous linear coastlines with the same orientation (Figure 3). Volcanic lineaments and linear canyons with a somewhat similar orientation, though closer to N150, are also observed in the central part of the island, e.g., on the northern and southern sectors of Fogo, and north of Furnas. Some of these features, especially north of Fogo, have been attributed to a graben structure [*Carvalho et al.*, 2006], but we did not find clear field evidence for major faults, and the topography does not show significant offset in this area (Figure 3). In contrast, we observed evidence of numerous faults with a similar strike in the Povoação depression. We especially report for the first time two major normal faults with opposite dip, which affect a volcanic succession dated around 450 ka [*Sibrant et al.*, 2013b; *Sibrant*, 2014; *Sibrant et al.*, 2015b]. These faults bound a graben, the central part of which is offset downward by at least 125 m (Figure 6). This graben is not obvious in the DEM, because it has been significantly filled by both conglomerates and young and thick ignimbritic flows, dated at 60 ka [*Sibrant*, 2014; *Sibrant et al.*, 2015b]. In previous studies, the Povoação depression was interpreted as a caldera, associated with pyroclastic flows and ignimbrites presumably erupted from a volcano, the so-called Povoação Volcano [*Moore*, 1990]. However, this appears rather unlikely, because the morphology and the age of the northern and southern flanks of the inferred volcano are very different [*Sibrant et al.*, 2015b]. The lava flows from the upper northern flank are circa 750 ka in age and represent a part of the Nordeste complex, whereas the lavas from the base of the lava succession range in age between 500 ka and 250 ka despite their lower position. This difference in age, together with morphologic and offshore data (bathymetry and seismic profiles) led *Sibrant et al.* [2015b] to conclude that the main axial E-W scarp results from a catastrophic *S*-directed large-scale collapse, which was later filled by lava flows presently cropping out in the Povoação depression. This means that the Povoação depression is not a volcano with a conical shape. Moreover, a caldera collapse generally produces concentric fault patterns [*Walker*, 1984; *Walter and Troll*, 2001; *Kinvig et al.*, 2009], even in areas dominated by regional tectonics [*Francis et al.*, 1978; *Acocella et al.*, 2004] and/or volcanic deposits associated with the catastrophic event. *Duncan et al.* [1999] argued that the ignimbrites, which they called the Povoação ignimbrite formation (PIF), are the products of the largest explosive eruption of the neighboring Furnas volcano and were not produced by a "Povoação volcano." Thus, none of our observations indicate the presence of concentric faults, and no pyroclastic deposits other than the PIF were observed within the structure. Considering all the evidence, we suggest that the depression of Povoação is not a caldera. Instead, we suggest, based on the new proposed evolution of the Nordeste VC [*Sibrant et al.*, 2015b] and this study, that the volcanism has been affected by a graben-oriented N150, which was subsequently filled by at least 25 m of ignimbrite (PIF) from a Furnas volcano event, which smoothed the topography. The current circular depression results from focused erosion processes and watershed configuration of the ignimbrite flow. Such structural control on erosion processes and watershed reconfiguration has been observed and described in other oceanic islands [*Gillot et al.*, 1994; *Hildenbrand et al.*, 2008b].

In contrast to the other trends, the N110 trend does not constitute linear coastlines or significant canyons or scarps, except in the southeastern part of São Miguel (Figure 3). Two linear scarps oriented N110 can be identified. These two scarps bound a linear topographic depression with a height of nearly 250 m (Figure 4). We suggest that this depression is a graben here called the Água Retorta Graben. Despite the relatively small topographic expression of the N110 trend in the global morphology of São Miguel, the N110 orientation represents one of two main trends of measured dykes and faults.

Finally, the two main structural trends (N110 and N150) measured in São Miguel [*Zbyszewski et al.*, 1959; *Moore*, 1990; the current study] are not the same as the main elongation directions of the island, which are along N80 and N130 azimuths. This reveals an angular deviation of 20–30° between the tectonic markers in the island and the main elongation directions of the island and the TR, i.e., a difference between the tectonics in the volcanic edifice (small scale) and in the underlying lithosphere (large scale). In São Miguel, fault and dyke orientations are shifted similarly to what has been described on other volcanoes in Hawaii [*Dieterich*, 1988; *Borgia*, 1994] and Madeira islands [*Klugel et al.*, 2005]. On São Miguel, the large central volcanoes and the strombolian cones indicate two orientations: N80 and N130, which coincide with the crustal/lithospheric trends. In contrast, faults and dykes show two different orientations, N110 and N150, which raises the question of which channels have been used by magma to reach the surface. The young strombolian edifices are basaltic and monogenetic, which indicates that the presence of a clear magmatic reservoir is not realistic. We thus infer that the magma has been transported directly through the lithosphere to the surface through the main large-scale channels [*Zanon*, 2015; *Zanon and Pimentel*, 2015]. From the fault and dyke data at the surface, we infer that the rotation of the tectonic trends observed between depth and surface should have a secondary origin. Many natural examples exist that show that structural trends change when there is a significant topographic relief, like a large volcanic cone, both in extensional [e.g., *de Vries and Merle*, 1996, Figure 1] and compressional [e.g., *Marques and Cobbold*, 2002, Figure 13] settings. It has been shown that the load of a volcanic edifice generates a local stress field that interferes with the regional stress field produced by far-field tectonics, and therefore, the tectonic structures reflect the sum of both stress fields [*de Vries and Merle*, 1996; *Pinel and Jaupart*, 2004; *Klugel et al.*, 2005]. This has been experimentally shown for different stress regimes and tectonic settings (e.g., *de Vries and Merle* [1996] for extensional tectonics and *Marques and Cobbold* [2002, 2006] for compressional settings). What the experimental works have shown is that the faults away from the volcanic edifice (produced by the far-field tectonics) rotate and cut across the volcanic edifice with a different trend (as a result of the local, volcano-induced stress field), which can deviate by as much as 60° with respect to the main regional trend. Based on natural and experimental evidence, we infer that the angular difference between large-scale trends and superficial structural trends in São Miguel results from the stresses imposed by the load of São Miguel's volcanic edifice on the far-field stresses. We therefore propose that the rotation of the tectonic markers between depth (large scale) and surface (small scale) is due to the load of the volcanic edifice. Consequently, the stresses from fault kinematics and dikes at the surface in the island also differ from the kinematics reported by *DeMets et al.* [2010] for the eastern TR: ENE-WSW extension from plate kinematics versus NE-SW here deduced from faults and dikes.

5.2. Variation in Distribution of the Tectonic Markers Across the Island

Our new structural data not only show that São Miguel is affected by the N110 and N150 dominant directions but also a newly recognized main N50 to N80 direction and an additional N20 subsidiary direction. Our measurements indicate a variation in the orientation of the major structures and faults and dikes, within 20 km only (from the eastern end of Nordeste to Furnas), from N110-dominated in the east to N150-dominated in the west. Three volcanic complexes constitute the eastern part of São Miguel: Nordeste, filling volcanism of Povoação, and Furnas [*Sibrant et al.*, 2015b]. As we discussed previously in section 5.1, the dip (Figures 3 and 4), the age, and the morphology of lavas making up the filling volcanism of Povoação indicate that this complex cannot be considered as an edifice, because the northern, western, and eastern flanks do not exist. Furthermore, if the structural (faults) and magmatic (dikes) patterns were produced by the large conical volcanic edifices, we should find radial patterns on the northern flanks of Nordeste, and all around Furnas, Fogo, and Sete Cidades, which is not the case. Therefore, radial structures in that area are not expected, so the measured trends must have a different explanation. In other words, distribution and orientation of faults and dykes is most likely induced by the regional deformation and should thus provide information on the TR. Recent bathymetric charts presented in *Weiß et al*. [2015a, 2015b, cf. Figure 12] show that the N110 and N150 structural trends measured onshore correspond to similar orientations recognized offshore. The bathymetric chart in their Figure 12 (and our Figure 9) shows approximately N90 to N110 normal faults offshore Zone 1 defined here (which corresponds in the offshore to the TR's NE shoulder) and approximately N140 normal faults offshore Zone 3 defined here (which corresponds in the offshore to the TR's SW shoulder). Besides being observed in eastern São Miguel, and also along the ESE and WNW ends of the TR, the N110-N120 azimuth is the orientation of most volcanic ridges in the Azores E of the MAR (e.g., Pico-Faial and São Jorge ridges). The kinematics of N110-N120 faults is typically normal with a dextral strike-slip component

as found in this study, consistent with the velocity vector of plate kinematics. The N140-N150 fault system can be found in São Miguel and offshore in the Povoação [*Weiß et al*., 2015a, 2015b] and Hirondelle Basins [e.g., *Hirn et al*., 1980]. In São Miguel the N140-N150 system occurs as mostly normal faults, but the fault plane solution for the 01.01.1980 shock indicates a rupture on a vertical N140-N150 fault with pure sinistral strike slip [*Hirn et al*., 1980].

The density of faults and dikes considerably decreases from east to west across the island. Moreover, it has been shown that deformation in the TR mostly occurs along one or two pairs of master faults that bound a rift with a generally flat bottom [e.g., *Searle*, 1980; *Vogt and Jung*, 2004]. Based on these two premises, we propose that the observed variation in fault and dyke distribution is due to the proximity of eastern São Miguel to the northern TR wall (where deformation is concentrated) and to the central location of western São Miguel in the TR (where deformation has not been detected). Moreover, *Sibrant et al.* [2015b] dated the volcanic activity in Nordeste between 800 and 750 ka, between 500 and 250 ka in Povoação, and less than 140 ka in Furnas volcano. Applying the principle of cross-cutting relationships, we infer that the faults and dykes cutting each of these volcanic complexes are younger than 750, 250, and 140 ka, respectively. The tectonic markers cut distinct volcanic complexes of different ages; however, the orientation and the stress field deduced from these tectonic markers are similar. Focal mechanisms of earthquakes along the Eurasia-Nubia plate boundary with nodal planes oriented N150 show close to NE-SW extension [*Borges et al*., 2007; *DeMets et al*., 2010]. The stress field deduced for Zones 2 and 3 is similar, with a $\sigma 3$ close to NE-SW. *DeMets et al.* [2010] also concluded that the stress field has not varied during the last 3 Myr, but we notice a variation in computed stress fields between Zones 2–3 and 1. Zones 1 and 2 are in the same edifice, so the variation between these two zones is probably not due to topographic effects (see discussion above) but in turn can be a local effect due to the position of São Miguel in the TR, especially its proximity to the northern master bounding fault of the TR.

São Miguel is not only located in the TR, and partly on its northern shoulder, but also at the inflection between two N130-N150 rift segments, connected by a N80 transform segment. These orientations coincide with the orientations of São Miguel: approximately N80 in the eastern two thirds of the island and N130 in the westernmost third. Based on the data reported in *DeMets et al.* [2010], on São Miguel's main trends, and on the new structural data, we propose that the eastern two thirds of São Miguel lie on top of a main transform fault oriented N70-N80, which connects two widely separated N130-N150 segments of the TR and is coincident with the orientation expected for TR-related transforms given the counterclockwise rotation of Nu relative to Eu. The N70-N80 fault system can also be recognized offshore the eastern end of São Miguel in the bathymetric chart shown in Figure 9. The variations in island shape and orientation of tectonic markers across the island reflect the local segmented shape of the TR, and the particular position of São Miguel inside the TR.

The tectonic structures are much more abundant near the TR wall than in the center of the island. However, the younger fissural systems in central and western São Miguel are elongated along the N80 and N130 directions, which means that even if the structural markers, such as faults or dikes, lack at the surface, the tectonic control at depth is still present. Given the paucity of faults and dykes in the western part of São Miguel, we propose that the tectonics induced by Nubia and Eurasia plate motions along the TR is mainly accommodated by the walls of the TR and not significantly by the central axis. Such different tectonic expression between bounding faults and inner parts of the TR also favors the development of grabens and normal faults and numerous dikes preferentially in the east. Moreover, the volcanoes localized in the middle of the rift are younger than volcanoes localized along the shoulder of the rift. Thus, the wall of the TR accommodates the structural pattern, whereas the magmatic pattern is accommodated by the deep rift axis. The Nordeste volcano represents the first stage of rift opening, where the volcanism is located along the shoulder, and the Sete Cidades indicates that the opening has advanced enough to localize volcanism in the middle of the TR.

Finally, information regarding the stress field variation between Zone 1 and Zones 2–3 suggests that the wall of the hyperslow Terceira Rift is constituted by pure normal faults and that the oblique extension of the TR develops toward the middle of the Rift.

5.3. Architecture of the Terceira Rift

Weiß et al. [2015a] present high-resolution images and two seismic profiles perpendicular to the South Hirondelle (NW of São Miguel) and Povoação Basins (SE of São Miguel). The images (Figure 9) show a graben morphology in the approximately 55 and 40 km wide rift valleys of the NW and SE basins, respectively. The

South Hirondelle Basin is bounded by major normal faults dipping to the NE in the SW wall, and to the SW in the NE wall. The basin floor is not all flat: the southern wall passes sharply into a flat basin floor, whereas the northern wall joins the basin floor through a gentle slope. Similarly to the South Hirondelle Basin, the NE wall of the Povoação Basin is made of several normal faults dipping to the SW. In contrast, the SW wall is dominated by three main normal faults dipping to the NE. From the seismic images, and according to *Weiß et al.* [2015a, 2015b], evidence has not been found for voluminous volcanism in the middle of the TR immediately close to São Miguel Island, either in the form of sediments covering old volcanic units or hosting intrusive volcanics. A few submarine volcanic cones are visible west of São Miguel, but they are considered to constitute parasitic volcanism scattered on the submarine flank of the Sete Cidades volcanic complex, rather than a major volcanic field controlled by large lithospheric faults.

The width of the relative flat bottoms of the South Hirondelle and Povoação Basins is between 17 km and 15 km (Figure 9), which are the values we use here to estimate when the TR has likely initiated. From seismic reflection profiles, we now know the morphology of the rift, the number of normal faults, their dip, and their vertical offset. Two published focal depths of 12 ± 5 and 15 ± 5 km [*Grimison and Chen*, 1986; *Dias et al.*, 2007] for earthquakes in this part of the TR give a fairly good estimation of the thickness of the brittle seismogenic lithosphere. With a thickness of the brittle crust of 15 km, we can calculate the width at the bottom of the basins using simple trigonometry. Using a mean dip angle of faults and the vertical offset, the result indicates a width at the bottom of around 19 km and comprised between 12 and 17 km for the NW and SE basin, respectively. This geometrical estimation of the width at the bottom of the TR is similar to the current topographic width obtained from the bathymetry. Therefore, the absence of voluminous volcanism at the bottom of the TR (seismic profiles) and our calculations suggest that rifting at the TR has been accommodated solely by normal faulting, without any, or only minor, seafloor spreading. Significant spreading would make the TR much wider than estimated and observed.

Given that the TR is seemingly opening without spreading (calculations with spreading are therefore not necessary), the horizontal extension can be measured from the seismic profile and from the dip of the faults (Figure S5). The total horizontal extension is estimated between 7.8 and 12 km for the South Hirondelle Basin and between 6.5 and 9 km for the Povoação Basin. The present extension rate orthogonal to the TR is of approximately 4.5 mm/yr [*DeMets et al.*, 2010], which indicates that the TR should have initiated between 1.4 Ma and 2.7 Ma ago, in fairly good agreement with the recent estimates obtained independently by *Vogt and Jung* [2004] and *Sibrant et al.* [2013a].

The axial morphology of hyperslow rifts like the TR is a function of two main competing processes that vary in time and space: the volcanic activity, which results in the construction of relatively smooth features, and faulting/rifting, which results in the creation of rough, linear features at many scales. The width of a rift, its structure, and the style of volcanism within it therefore change considerably with opening rate.

Morphological studies on mature slow ridges, like the MAR, have shown that there are interactions between the morphology of rift valleys, mantle upwelling, and rifting processes [*Perfit and Chadwick*, 1998]. A rift valley with shallow graben morphology can be interpreted as nonvolcanic, or sparsely magmatic (seamounts and islands), with dominant tectonic extension [*Perfit and Chadwick*, 1998]. Even if the existence of a plume below the Azores is still debated [e.g., *Bonatti*, 1990; *Silveira and Stutzmann*, 2002; *Métrich et al.*, 2014], the emplacement and the evolution of the Azores volcanism is largely controlled by competing tectonic and volcanic processes and mostly by the regional deformation due to plate kinematics [e.g., *Lourenço et al.*, 1998; *Hildenbrand et al.*, 2008a, 2012, 2013, 2014]. *Montési and Behn* [2007] showed that the rate of expansion along an oceanic ridge has a direct influence on the thickness of the crust and the thermal structure of the ridge. If the extension rate is less than 6.5 mm/yr, the volcanism along the axis is not continuous. As the TR shows an extension rate between 4 mm/yr [*DeMets et al.*, 2010] and 3.5 mm/yr [*Marques et al.*, 2013, 2014a], it is thus not surprising to have a discontinuous volcanism. For example, along the Ethiopian rift the volcanism in the magmatic segments started circa 1.6 Myr ago, and most flows emanated first as main shield volcanoes, which were later followed by fissures and small cinder cones with some differentiation [*Boccaletti et al.*, 1999]. In oceanic rifts, the along axis segmentation is defined by dike injection and faulting with an axial valley and flank morphology [e.g., *Batiza*, 1996]. Ultraslow spreading ridges such as the South West Indian Ridge show a more extreme focusing of melt, with the construction of large central volcanoes at the center of some segments, while others are relatively magmatically starved [*Cannat et al.*, 1999; *Dick et al.*, 2003]. The TR and other

slow opening oceanic ridges (as the SWIR or the Gakkel ridge) show some similarities in the position of the volcanism. Our estimation indicates that no significant spreading has occurred along the current TR, and volcanism is concentrated in main central-type volcanoes spaced regularly along the TR.

Finally, the N50 to N80 fault system newly put in evidence in São Miguel is not a direction commonly described in the Azores (Zone 4, Figure 4). The absence of N50 fault planes favorable for measurement of striations limited the determination of fault kinematics. However, focal mechanisms of earthquakes in central Azores (Figure 7, shocks of 01.01.1980 and 09.07.1998) show two subvertical nodal planes, one of which is oriented approximately N60 [*Borges et al.*, 2007; *Marques et al.*, 2014b]. Similar trends have been recently recognized in Graciosa [*Sibrant et al.*, 2014, 2015c], São Jorge [*Silva et al.*, 2012b], and in the 09.07.1998 Faial earthquake [*Marques et al.*, 2014b]. Thus, although not conspicuous within the islands, the N60 to N80 trend seems to be important for the recent tectonics of the Nubia-Eurasia plate boundary. The N60 strike slip fault system is located between islands, as in the diffuse Nubia/Eurasia plate boundary (between the TR and the Pico-Faial ridge), or where the direction of the TR changes. This is the case of the São Miguel region, where the TR trend changes from N130 NW of São Miguel (Hirondelle Basin and western third of São Miguel), to N80 in São Miguel eastern two thirds, and to N150 SE of São Miguel (Povoação Basin, Figures 8 and 9). *DeMets et al.* [2010] in the model of the plate velocity configuration predicted the presence of such N80-N60 fault system, as a transform direction related to the TR (N80 at the eastern end and N60 at the western end of the TR—Figure 1). The counterclockwise rotation of Nubia relative to Eurasia produces pure dextral strike slip in the Gloria Fault and extension in the Azores region, with a trend varying from N80 to N60 at the eastern and western ends of the TR, respectively (Figure 1). The schematic interpretation based on plate kinematics and our new structural observations, mostly the newly recognized N70-N80 fault system, show the tectonic and kinematic configuration around São Miguel (Figure 7). In this interpretation, we infer dextral strike slip in the São Miguel transform (indicated by the white half arrows), similarly to the Gloria Fault, as the result of opening in the N80 direction in the TR, NW and SE of São Miguel, as indicated by plate kinematics, and represented by the white arrows.

Moreover, based on structural data, measured ground motion and modeling, *Marques et al.* [2014b] showed that the N60 fault plane solution of the 1998 earthquake can be associated with the Nubia-Eurasia diffuse plate boundary and can be a transform fault. Therefore, we conclude that the eastern two thirds of São Miguel are most likely lying on a TR-related transform fault linking two widely separated segments of the TR (Figure 7), which is reflected at the surface by the alignment of the major Nordeste, Furnas, and Fogo volcanic edifices, by faults offshore east São Miguel, and by structural lineaments, including the smaller-scale N50 trending faults and dykes measured in this study.

Geological evidence has suggested that volcanism may occur along transform faults that offset first-order segments of fast mid-oceanic ridges [*Searle*, 1983; *Lonsdale*, 1986; *Lowrie et al.*, 1986; *Fornari et al.*, 1989; *Hekinian et al.*, 1992; *Hekinian et al.*, 1995; *Perfit et al.*, 1996; *Wendt et al.*, 1999; *Karson et al.*, 2002]. In contrast, the TR does not show observable along-axis spreading or fast opening rates. Recent magma production/extraction has been largely controlled by regional extension/transtension and focused along large tectonic structures (volcanic ridges inside grabens, like the Pico-Faial and São Jorge ridges), or at the intersection of major faults inside the TR (Graciosa, Terceira, and São Miguel), which appear to provide preferential and focused magmatic conduits for central-type volcanoes. Therefore, we conclude that the volcanism in São Miguel is by no means related directly to the here-proposed São Miguel transform. The role of the transform would be to facilitate the ascent of magma to the surface, and its eruption as central-type volcanoes, due to easier conduits made by fault intersections (TR fault system and São Miguel transform fault system).

6. Conclusions

Given that the TR is an active hyperslow rift, which comprises part of the current Eurasia-Nubia plate boundary, and that São Miguel Island spreads across the entire width of the TR, the study of São Miguel is crucial because it allows characterizing the way deformation has been accommodated across the TR.

From DEM and structural data, including new measurements of 380 faults and dikes, and available geophysical and bathymetric results, we conclude the following:

1. The eastern part of São Miguel comprises two newly recognized grabens: the Água Retorta and the Povoação grabens, oriented N110 and N150, respectively.

2. There is a rotation between the large-scale trends and the trends of the measured tectonic markers in the island, most likely due to a loading effect by the volcanic edifice(s).
3. Tectonic markers are much more abundant in the eastern part of the island relative to the central and western parts.
4. The orientation and distribution of faults and dikes indicate that eastern São Miguel comprises the TR's northern boundary, and the relative paucity of major faults at the surface in central and western São Miguel suggests that rifting is mostly concentrated at the master faults bounding the TR.
5. The initiation of the eastern part of the TR in the vicinity of São Miguel began probably between 1.4 and 2.7 Ma, and the rifting process has most likely did not include appreciable seafloor spreading.
6. The western two thirds of São Miguel have most likely grown on a TR-related N80 transform separating two main segments of the TR-trending N130 (NW of São Miguel) and N150 (SE of São Miguel), which we here coin the São Miguel transform.
7. Ultraslow rifts are typically very poor in magmatism, and rifting is preferentially concentrated along bounding master faults. This seems to be the case of the TR, in the middle of which tectonics seems to be much attenuated, and volcanism is concentrated in a few large volcanic edifices regularly spaced along the rift, and seemingly at the intersection of major faults.

Acknowledgments

Data supporting Figure 4 are available in Data Set S1 or by contacting the corresponding author. The authors thank B. Weiß for providing us the bathymetric map and seismic profiles around São Miguel. This is a contribution to Project MEGAHazards, funded by FCT, Portugal (PTDC/CTE-GIX/108149/2008). A.C.G. Costa benefitted from a PhD scholarship funded by Fundação para a Ciência e a Tecnologia Portugal (SFRH/BD/68983/2010). F.O. Marques was awarded a Sabbatical fellowship by FCT, Portugal (SFRH/BSAB/1405/2014). A.L.R. Sibrant benefitted from funding by the French CNRS-INSU and by French ANR (project RHUM-RUM). The manuscript has been improved, thanks to the constructive comments of the Associate Editor and anonymous reviewers. This is LGMT contribution 131.

References

Acocella, V., R. Funiciello, E. Marotta, G. Orsi, and S. DeVita (2004), The role of extensional structures on experimental calderas and resurgence, *J. Volcanol. Geotherm. Res.*, *129*, 199–217, doi:10.1016/S0377-0273(03)00240-3.

Agostinho, J. (1931), The volcanoes of the Azores Islands, *Bull. Volcanol.*, *8*, 123–138.

Angelier, J. (1984), Tectonic analysis of fault slip data sets, *J. Geophys. Res.*, *89*(B7), 5835–5848, doi:10.1029/JB089iB07p05835.

Angelier, J. (1994), Fault slip analysis and palaeostress reconstruction, in *Continental Deformation*, edited by P. L. Hancock, pp. 53–100, Pergamon Press, Oxford.

Appelgate, B., and A. N. Shor (1994), The northern Mid-Atlantic and Reykjanes Ridges: Spreading center morphology between 55°50′N and 63°00′N, *J. Geophys. Res.*, *99*(B9), 17,935–17,956, doi:10.1029/93JB03459.

Argus, D., R. Gordon, C. DeMets, and S. Stein (1989), Closure of the Africa–Eurasia–North America plate motion circuit and tectonics of the Gloria fault, *J. Geophys. Res.*, *94*, 5585–5602, doi:10.1029/JB094iB05p05585.

Bache, F., N. Mortimer, R. Sutherland, J. Collot, P. Rouillard, V. Stagpoole, and A. Nicol (2013), Seismic stratigraphic record of transition from Mesozoic subduction to continental breakup in the Zealandia sector of eastern Gondwana, *Gondwana Res.*, *26*(3-4), doi:10.1016/j.gr.2013.08.012.

Batiza, R. (1996), Magmatic segmentation at mid-ocean ridges: A review, in *Tectonic, Magmatic, Hydrothermal, and Biological Segmentation of Mid Ocean Ridges*, *Geological Society of London, Special Publication*, vol. 118, edited by C. MacLeod et al., pp. 39–49, Geol. Soc., London.

Bezzeghoud, M., C. Adam, E. Buforn, J. F. Borges, and B. Caldeira (2014), Seismicity along the Azores-Gibraltar region and global plate kinematics, *J. Seismol.*, *18*, 205–220.

Boccaletti, M., R. Mazzuoli, M. Bonini, T. Trua, and B. Abebe (1999), Plio-Quaternary volcanotectonic activity in the northern sector of the Main Ethiopian rift: Relationships with oblique rifting, *J. Afr. Earth Sci.*, *29*, 679–698.

Bonatti, E. (1990), Not so hot "hot spots" in the oceanic mantle, *Science*, *250*, 107–111, doi:10.1126/science.250.4977.107.

Borges, J. F., M. Bezzeghoud, E. Buforn, C. Pro, and A. Fitas (2007), The 1980, 1997 and 1998 Azores earthquakes and some seismo-tectonic implications, *Tectonophysics*, *435*, 37–54, doi:10.1016/j.tecto.2007.01.008.

Borgia, A. (1994), Dynamic basis of volcanic spreading, *J. Geophys. Res.*, *99*(B9), 17,791–17,804, doi:10.1029/94JB00578.

Buforn, E., A. Udias, and M. A. Colombas (1988), Seismicity, source mechanisms and seismotectonics of the Azores-Gibraltar plate boundary, *Tectonophysics*, *152*, 89–118.

Buforn, E., M. Bezzeghoud, A. Udias, and C. Pro (2004), Seismic sources on the Iberia-African plate boundary and their tectonic implications, *Pure Appl. Geophys.*, *161*, 623–646.

Byerlee, J. D. (1967), Frictional characteristics of granite under high confining pressure, *J. Geophys. Res.*, *72*, 3639–3648, doi:10.1029/JZ072i014p03639.

Calais, E., C. DeMets, and J.-M. Nocquet (2003), Evidence for a post-3.16-Ma change in Nubia–Eurasia–North America plate motions?, *Earth Planet. Sci. Lett.*, *216*, 81–92.

Cannat, M., C. Rommevaux-Jestin, D. Sauter, C. Deplus, and V. Mendel (1999), Formation of the axial relief at the very slow spreading Southwest Indian Ridge (49° to 69°E), *J. Geophys. Res.*, *104*(B10), 22,825–22,843, doi:10.1029/1999JB900195.

Cannat, M., C. Rommevaux-Jestin, and H. Fujimoto (2003), Melt supply variations to a magma-poor ultra-slow spreading ridge (Southwest Indian Ridge 61° to 69°E), *Geochem. Geophys. Geosyst.*, *4*(8), 9104, doi:10.1029/2002GC000480.

Carvalho, M. R., V. H. Forjaz, and C. Almeida (2006), Chemical composition of deep hydrothermal fluids in the Ribeira Grande geothermal field (São Miguel), *J. Volcanol. Geotherm. Res.*, *156*(1–2), 116–134, doi:10.1016/j.jvolgeores.2006.03.015.

Casalbore, D., C. Romagnoli, A. Pimentel, R. Quartau, D. Casas, G. Ercilla, A. Hipolito, A. Sposato, and F. L. Chiocci (2015), Volcanic, tectonic and mass-wasting processes offshore Terceira Island (Azores) revealed by high-resolution seafloor mapping, *Bull. Volcanol.*, *77*, 24, doi:10.1007/s00445-015-0905-3.

Coalkey, B., and J. Cochran (1998), Gravity evidence of very thin crust at the Gakkel Ridge (Arctic Ocean), *Earth Planet. Sci. Lett.*, *162*, 81–95.

Corti, G. (2009), Continental rift evolution: From rift initiation to incipient break-up in the Main Ethiopian Rift, East Africa, *Earth Sci. Rev.*, *96*(1–2), 1–53.

Costa, A. C. G., F. O. Marques, A. Hildenbrand, A. L. R. Sibrant, and C. M. S. Catita (2014), Large-scale flank collapses in a steep volcanic ridge: Pico-Faial Ridge, Azores Triple Junction, *J. Volcanol. Geotherm. Res.*, *272*, 111–125.

de Vries, B. W., and O. Merle (1996), The effect of volcanic constructs on rift fault patterns, *Geology*, *24*, 643–646.

DeMets, C., R. Gordon, A. Argus, and A. Stein (1990), Current plate motions, *Geophys. J. Int.*, *101*, 425–478.

DeMets, C., R. G. Gordon, and D. F. Argus (2010), Geologically current plate motions, *Geophys. J. Int.*, *181*, 1–80, doi:10.1111/j.1365-246X.2009.04491.x.
Detrick, B., H. D. Needham, and V. Renard (1995), Gravity anomalies and crustal thickness variations along the Mid-Atlantic Ridge between 10°N and 40°N, *J. Geophys. Res.*, *100*, 3767–3778, doi:10.1029/94JB02649.
Dias, N. A., L. Matias, N. Lourenço, J. Madeira, F. Carrilho, and J. L. Gaspar (2007), Crustal seismic velocity structure near Faial and Pico Islands (Azores), from local earthquake tomography, *Tectonophysics*, *445*(3–4), 301–317.
Dick, H. J. B., J. Lin, and H. Schouten (2003), Ultra slow spreading—A new class of ocean ridge, *Nature*, *426*, 405–412.
Dieterich, J. H. (1988), Growth and persistence of Hawaiian volcanic rift zones, *J. Geophys. Res.*, *93*, 4258–4270, doi:10.1029/JB093iB05p04258.
Driscoll, N., and G. Karner (1998), Lower crustal extension across the Northern Carnarvon basin, Australia: Evidence for an eastward dipping detachment, *J. Geophys. Res.*, *103*, 4975–4991, doi:10.1029/97JB03295.
Duncan, A. M., G. Queiroz, J. E. Guest, P. D. Cole, N. Wallenstein, and J. M. Pacheco (1999), The Povoação Ignimbrite, Furnas Volcano, São Miguel, Azores, *J. Volcanol. Geotherm. Res.*, *92*(1–2), 55–65, doi:10.1016/S0377-0273(99)00067-0.
Duncan, R. A., and I. McDougall (1976), Geologically current plate motions, *Geophys. J. Int.*, *181*, 1–80.
Elliott, T., J. Blichert-Toft, A. Heumann, G. Koetsier, and V. Forjaz (2007), The origin of enriched mantle beneath São Miguel, Azores, *Geochim. Cosmochim. Acta*, *71*, 219–240.
Fernandes, R. M. S., B. A. C. Ambrosius, R. Noomen, L. Bastos, M. J. R. Wortel, W. Spakman, and R. Govers (2003), The relative motion between Africa and Eurasia as derived from ITRF2000 and GPS data, *Geophys. Res. Lett.*, *30*(16), 1828, doi:10.1029/2003GL017089.
Fernandes, R. M. S., L. Bastos, B. A. C. Ambrosius, R. Noomen, S. Matheussen, and P. Baptista (2004), Recent geodetic results in the Azores Triple Junction region, *Pure Appl. Geophys.*, *161*, 683–699.
Fernandes, R. M. S., L. Bastos, J. M. Miranda, N. Lourenço, B. A. C. Ambrosius, R. Noomen, and W. Simons (2006), Defining the plate boundaries in the Azores region, *J. Volcanol. Geotherm. Res.*, *156*, 1–9.
Forjaz, V. H. (1993), *Tectonic Map of S. Miguel, 2 Sheets at 1:50000 Scale*, Centro de Vulcanologia da Universidade dos Açores, Ponta Delgada.
Forjaz, V. H. (1997), *Alguns Vulcões Da Ilha De S. Miguel*, 160 pp., Observatorio Vulcanologico e Geotérmico dos Açores, Ponta Delgada.
Forjaz, V. H., et al. (2004), *Basic Atlas of the Azores (in Portuguese)*, edited by V. H. Forjaz, 112 pp., Observatorio Vulcanologico e Geothermico dos Açores, Ponta Delgada.
Fornari, D. J., M. H. Edwards, D. G. Gallo, J. A. Madsen, M. R. Perfit, and A. N. Shor (1989), Structure and topography of the Siqueiros trasform fault system: Evidence for the development of intra-transform spreading centers, *Mar. Geophys. Res.*, *11*, 263–299.
Francheteau, J., and R. D. Ballard (1983), The East Pacific Rise near 21°N, 13″, and 20°S: Inferences from along-strike variability of axial processes of the mid-ocean ridges, *Earth Planet. Sci. Lett.*, *64*, 93–116.
Francis, P. W., M. Hammill, G. Kretzschmar, and R. S. Thorpe (1978), The Cerro Galan Caldera, North west Argentina and its tectonic setting, *Nature*, *274*, 749–751.
Gandino, A., M. Guidi, C. Merlo, L. Mete, R. Rossi, and L. Zan (1985), Preliminary model of the Ribeira Grande geothermal field (Azores Islands), *Geothermics*, *14*(1), 91–105.
Gente, P., J. Dyment, M. Maia, and J. Goslin (2003), Interaction between the Mid Atlantic ridge and the Azores hotspot during the last 85 Myr: Emplacement and rifting of the hotspot derived plateaus, *Geochem. Geophys. Geosyst.*, *8*, Q03013, doi:10.1029/2006GC001318.
Georgen, J. E., and R. D. Sankar (2010), Effects of ridge geometry on mantle dynamics in an oceanic triple junction region: Implications for the Azores Plateau, *Earth Planet. Sci. Lett.*, *298*, 23–34.
Gillot, P. Y., J. C. Lefevre, and P. E. Nativel (1994), Model for the structural evolution of the volcanoes of Reunion island, *Earth Planet. Sci. Lett.*, *122*, 291–302, doi:10.1016/0012-821X(94)90003-5.
Grimison, N. L., and W. P. Chen (1986), The Azores-Gilbraltar plate boundary: Focal mechanisms, depths of earthquakes, and their tectonic implications, *J. Geophys. Res.*, *91*(B2), 2029–2047, doi:10.1029/JB091iB02p02029.
Haase, K. M., and C. Beier (2003), Tectonic control of ocean island basalt source on São Miguel, Azores?, *Geophys. Res. Lett.*, *30*(16), 1856, doi:10.1029/2003GL017500.
Hekinian, R., D. Bideau, M. Cannat, J. Francheteau, and R. Hébert (1992), Volcanic activity and crust-mantle exposure in the ultrafast Garrett transform fault near 13°28′S in the Pacific, *Earth Planet. Sci. Lett.*, *108*, 259–275.
Hekinian, R., D. Bideau, R. Hébert, and Y. Niu (1995), Magmatism in the Garrett transform fault (East Pacific Rise near 13°27′S), *J. Geophys. Res.*, *100*, 10,163–10,185, doi:10.1029/94JB02125.
Henk, A. (2006), Stress and strain during fault-controlled lithospheric extension-insights from numerical experiments, *Tectonophysics*, *415*, 39–55.
Hildenbrand, A., P. Y. Gillot, and I. LeRoy (2004), Volcano-tectonic and geochemical evolution of an oceanic intra-plate volcano: Tahiti-Nui (French Polynesia), *Earth Planet. Sci. Lett.*, *217*(3), 349–365.
Hildenbrand, A., P. Madureira, F. O. Marques, I. Cruz, B. Henry, and P. Silva (2008a), Multi-stage evolution of a sub-aerial volcanic ridge over the last 1.3 Myr: S. Jorge Island, Azores Triple Junction, *Earth Planet. Sci. Lett.*, *273*, 289–298.
Hildenbrand, A., P. Y. Gillot, and C. Marlin (2008b), Geomorphological study of long term erosion on a tropical volcanic ocean island: Tahiti-Nui (French Polynesia), *Geomorphology*, *93*, 460–481, doi:10.1016/j.geomorph.2007.03.012.
Hildenbrand, A., F. O. Marques, A. C. G. Costa, A. L. R. Sibrant, P. F. Silva, B. Henry, J. M. Miranda, and P. Madureira (2012), Reconstructing the architectural evolution of volcanic islands from combined K/Ar, morphologic, tectonic, and magnetic data: The Faial Island example (Azores), *J. Volcanol. Geotherm. Res.*, *241-242*, 39–48, doi:10.1016/j.jvolgeores.2012.06.019.
Hildenbrand, A., F. O. Marques, A. C. G. Costa, A. L. R. Sibrant, P. M. F. Silva, B. Henry, J. M. Miranda, and P. Madureira (2013), Reply to the comment by Quartau and Mitchell on reconstructing the architectural evolution of volcanic islands from combined K/Ar, morphologic, tectonic and magnetic data: The Faial Island example (Azores), J. Volcan. Geotherm. Res., 241-242, 39-48, by Hildenbrand et al., (2012), *J. Volcanol. Geotherm. Res.*, *255*, 127–130.
Hildenbrand, A., D. Weis, P. Madureira, and F. O. Marques (2014), Recent plate re-organization at the Azores Triple Junction: Evidence from new geochemical and geochronological data on Faial, S. Jorge and Terceira volcanic islands, *Lithos*, *210-211*, 27–39.
Hirn, A., H. Haessler, P. Hoang Trong, G. Wittlinger, and L. A. Mendes Victor (1980), Aftershock sequence of the January 1st, 1980, earthquake and present-day tectonics in the Azores, *Geophys. Res. Lett.*, *7*, 501–504, doi:10.1029/GL007i007p00501.
Jiménez-Munt, I., and A. M. Negredo (2003), Neotectonic modelling of the western part of the Africa-Eurasia plate boundary: From the Mid-Atlantic ridge to Algeria, *Earth Planet. Sci. Lett.*, *205*, 257–271.
Johnson, C. L., J. R. Wijbrans, C. G. Constable, J. Gee, H. Staudigel, L. Tauxe, V. H. Forjaz, and M. Salgueiro (1998), $^{40}Ar/^{39}Ar$ ages and paleomagnetism of São Miguel Lavas, Azores, *Earth Planet. Sci. Lett.*, *160*(3–4), 637–649, doi:10.1016/S0012-821X(98)00117-4.
Karson, J. A., M. A. Tivey, and J. R. Delaney (2002), Internal structure of uppermost oceanic crust along the Western Blanco Transform Scarp: Implications for subaxial accretion and deformation at the Juan de Fuca Ridge, *J. Geophys. Res.*, *107*, 2181, doi:10.1029/2000JB000051.

Kinvig, H. S., A. Geyer, and J. Gottsmann (2009), On the effect of crustal layering on ring-fault initiation and the formation of collapse calderas, *J. Volcanol. Geotherm. Res.*, *186*, 293–304, doi:10.1016/j.jvolgeores.2009.07.007.
Kiratzi, A. A., and C. B. Papazachos (1995), Active crustal deformation from the Azores Triple Junction to the Middle East, *Tectonophysics*, *243*, 1–24.
Klugel, A., T. R. Walter, S. Schwarz, and J. Gelmacher (2005), Gravitational spreading causes en-echelon diking along a rift zone of Madeira Archipelago: An experimental approach and implications for magma transport, *Bull. Volcanol.*, *68*(1), 37–46.
Krause, D. C., and N. D. Watkins (1970), North Atlantic crustal genesis in the vicinity of the Azores, *Geophys. J. R. Astron. Soc.*, *19*, 261–283.
Larrea, P., J. R. Wijbrans, C. Galé, T. Ubide, M. Lago, Z. França, and E. Widom (2014), $^{40}Ar/^{39}Ar$ constraints on the temporal evolution of Graciosa Island, Azores (Portugal), *Bull. Volcanol.*, *76*, 796, doi:10.1007/s00445-014-0796-8.
Laughton, A. S., and R. B. Whitmarsh (1974), The Azores-Gibraltar plate boundary, in *Geodynamics of Iceland and the North Atlantic Area*, edited by L. Kristjansson, pp. 63–81, Reidel, Dordrecht, Netherlands.
Laughton, A. S., R. B. Whitmarsh, J. S. M. Rusby, M. L. Somers, J. Revie, B. S. McCartney, and J. E. Nafe (1972), A continuous East-West Fault on the Azores-Gibraltar Ridge, *Nature*, *237*, 217–220.
Lonsdale, P. F. (1986), East Pacific Rise from Siqueiros to Orozco fracture zones; along-strike continuity of axial neovolcanic zones and structure and evolution of overlapping spreading centers; discussion, *J. Geophys. Res.*, *91*, 10,493–10,499, doi:10.1029/JB091iB10p10493.
Lourenço, N., J. F. Luís, J. M. Miranda, A. Ribeiro, and L. A. M. Victor (1998), Morpho-tectonic analysis of the Azores volcanic plateau from new bathymetric compilation of the area, *Mar. Geophys. Res.*, *20*, 141–156, doi:10.1023/A:1004505401547.
Lowrie, A., C. Smoot, and R. Batiza (1986), Are oceanic fracture zones locked or strong and weak? New evidence for volcanic activity and weakness, *Geology*, *14*, 242–245.
Luís, J. F., and J. M. Miranda (2008), Reevaluation of magnetic chrons in the North Atlantic between 35°N and 47°N: Implications for the formation of the Azores Triple Junction and associated plateau, *J. Geophys. Res.*, *113*, B10105, doi:10.1029/2007JB005573.
Luís, J. F., J. Miranda, A. Galdeano, and P. Patriat (1998), Constraints on the structure of the Azores spreading center from gravity data, *Mar. Geophys. Res.*, *20*, 157–170, doi:10.1023/A:1004698526004.
MacDonald, K. C. (1982), Mid-ocean ridges: Fine scale tectonic, volcanic and hydrothermal processes within the plate boundary zone, *Annu. Rev. Earth Planet. Sci. Lett.*, *10*, 155–190.
Machado, F. (1959), Submarine pits of the Azores plateau, *Bull. Volcanol.*, *21*, 109–116.
Magde, L., D. Sparks, and R. Detrick (1997), The relationship between buoyant mantle flow, melt migration, and gravity bull's eyes at the Mid-Atlantic Ridge between 33°N and 35°N, *Earth Planet. Sci. Lett.*, *148*, 59–67.
Malinverno, A., and R. A. Pockalny (1990), Abyssal Hill topography as an indicator of episodicity in crustal accretion and deformation, *Earth Planet. Sci. Lett.*, *99*, 154–169.
Marques, F. O., and P. R. Cobbold (2002), Topography as a major factor in the development of arcuate thrust belts: Insights from sandbox experiments, *Tectonophysics*, *348*, 247–268.
Marques, F. O., and P. R. Cobbold (2006), Effects of topography on the curvature of fold-and-thrust belts during shortening of a 2-layer model of continental lithosphere, *Tectonophysics*, *415*, 65–80.
Marques, F. O., J. C. Catalão, C. DeMets, A. C. G. Costa, and A. Hildenbrand (2013), GPS and tectonic evidence for a diffuse plate boundary at the Azores Triple Junction, *Earth Planet. Sci. Lett.*, *381*, 177–187.
Marques, F. O., J. C. Catalão, C. DeMets, A. C. G. Costa, and A. Hildenbrand (2014a), Corrigendum to "GPS and tectonic evidence for a diffuse plate boundary at the Azores Triple Junction" [Earth Planet. Sci. Lett. 381 (2013) 177–187], *Earth Planet. Sci. Lett.*, *387*, 1–3.
Marques, F. O., J. Catalão, A. Hildenbrand, A. C. G. Costa, and N. A. Dias (2014b), The 1998 Faial earthquake, Azores: Evidence for a transform fault associated with the Nubia-Eurasia plate boundary?, *Tectonophysics*, *633*, 115–125.
Marques, F. O., J. Catalão, A. Hildenbrand, and P. Madureira (2015), Ground motion and tectonics in the Terceira Island: Tectonomagmatic interactions in an oceanic rift (Terceira Rift, Azores Triple Junction), *Tectonophysics*, *651–652*, 19–34, in press.
McKee, E. H., and R. B. Moore (1992), Potassium–argon dates for trachytic rocks on São Miguel, Azores, *Isochron West*, *58*, 9–11.
McKenzie, D. (1972), Active tectonics of the Mediterranean region, *Geophys. J. R. Astron. Soc.*, *30*, 109–185.
McKenzie, D. P. (1970), The plate tectonics of the Mediterranean region, *Nature*, *226*, 239–243.
Mendes, V. B., J. Madeira, A. Brum da Silveira, A. Trota, P. Elosegui, and J. Pagarete (2013), Present-day deformation in São Jorge Island, Azores, from episodic GPS measurements (2001–2011), *Adv. Space Res.*, *51*, 1581–1592.
Métrich, N., V. Zanon, L. Créon, A. Hildenbrand, M. Moreira, and F. O. Marques (2014), Is the "Azores hotspot" a wetspot? Insights from the geochemistry of fluid and melt inclusions in olivine of Pico basalts, *J. Petrol.*, *55*, 377–393.
Michael, P. J., et al. (2003), Magmatic and amagmatic seafloor generation at the ultraslow-spreading Gakkel ridge, Arct, Ocean, *Nature*, *423*, 956–961.
Miranda, J. M., et al. (1998), Tectonic setting of the Azores Plateau deduced from OBS survey, *Mar. Geophys. Res.*, *20*, 171–182.
Miranda, J. M., J. F. Luis, N. Lourenço, and J. Goslin (2014), Distributed deformation close to the Azores Triple "Point", *Mar. Geol.*, *355*, 27–35.
Montési, L. G., and M. D. Behn (2007), Mantle flow and melting underneath oblique and ultraslow mid-ocean ridges, *Geophys. Res. Lett.*, *34*, L24307, doi:10.1029/2007GL031067.
Moore, R. (1990), Volcanic geology and eruption frequency, S. Miguel, Azores, *Bull. Volcanol.*, *52*, 602–614, doi:10.1007/BF00301211.
Moore, R. (1991), Geologic map of São Miguel, Azores (scale 1: 50.000), *U.S.G.S.* MISC INV. map I-2007.
Moore, R., and M. Rubin (1991), Radiocarbon dates for lava flows and pyroclastic deposits on São Miguel, Azores, *Radiocarbon*, *33*(1), 151–164.
Moreira, V. S. (1985), Seismotectonics of Portugal and its adjacent area in the Atlantic, *Tectonophysics*, *117*, 85–96.
Morgan, W. J. (1971), Convection plumes in the lower mantle, *Nature*, *230*, 43–44.
Mutter, J. C., and J. A. Karson (1992), Structural processes at slow-spreading ridges, *Science*, *257*(5070), 627–634.
Nakamura, K., K. H. Jacob, and J. N. Davies (1977), Volcanoes as possible indicators of tectonic stress orientation—Aleoutians and Alaska, *Pure Appl. Geophys.*, *115*, 87–112.
Ortner, H., F. Reiter, and P. Acs (2002), Easy handling of tectonic data the programs TectonicVB for Mac and TectonicsFP for Windows, *Comput. Geosci.*, *28*, 1193–1200, doi:10.1016/S0098-3004(02)00038-9.
Ozawa, A., T. Tagami, and M. O. Garcia (2005), Unspiked K-Ar dating of the Honolulu rejuvenated and Ko'olau shield volcanism on O'ahu, Hawaii, *Earth Planet. Sci. Lett.*, *232*, 1–11.
Perfit, M. R., and W. C. Chadwick (1998), Magmatism at mid oceanic ridges: Constraints from volcanological and geochemical investigations in: Faulting and magmatism at mid ocean ridges, Buck, W. R., et al (eds), *AGU Geophys. Monogr.*, *106*, 59–116.
Perfit, M. R., et al. (1996), Recent volcanism in the Siqueiros transform fault: Picritic basaltic basalts and implications for MORB magma genesis, *Earth Planet. Sci. Lett.*, *141*, 91–108.
Pinel, V., and C. Jaupart (2004), Magma storage and horizontal dike injection beneath a volcanic edifice, *Earth Planet. Sci. Lett.*, *221*, 245–262.

Queiroz, G., J. M. Pacheco, J. L. Gaspar, W. P. Aspinall, J. E. Guest, and T. Ferreira (2008), The last 5000 years of activity at sete Cidades volcano (São Miguel island, Azores) implication for hazard assessment, *J. Volcanol. Geotherm. Res.*, *178*(3), 562–573, doi:10.1016/j.jvolgeores.2008.03.001.

Roman, A., and C. Jaupart (2014), The impact of a volcanic edifice on intrusive and eruptive activity, *Earth Planet. Sci. Lett.*, *408*, 1–8.

Schilling, J. G. (1975), Azores mantle blob: Rare earth evidence, *Earth Planet. Sci. Lett.*, *25*, 103–115.

Schilling, J. G. (1985), Upper mantle heterogeneities and dynamics, *Nature*, *314*, 62–67.

Searle, R. (1980), Tectonic pattern of the Azores spreading centre and triple junction, *Earth Planet. Sci. Lett.*, *51*(2), 415–434.

Searle, R. (1983), Multiple, closely spaced transform faults in fast-slipping fracture zones, *Geology*, *11*, 607–610.

Searle, R. C. (1976), Lithospheric structure of the Azores Plateau from Rayleigh-wave dispersion, *Geophys. J. R. Astron. Soc.*, *44*, 537–546.

Serpelloni, E., G. Vannucci, S. Pondrelli, A. Argnani, G. Casula, M. Anzidei, P. Baldi, and P. Gasperini (2007), Kinematics of the Western Africa–Eurasia plate boundary from focal mechanisms and GPS data, *Geophys. J. Int.*, *169*, 1180–1200.

Sibrant, A. L. R. (2014), Evolution of the Graciosa, S. Miguel and Santa Maria islands: Implications for the NU/EU plate boundary in the Azores, PhD thesis, Université Paris-Sud, France, 303 pp.

Sibrant, A. L. R., A. Hildenbrand, F. O. Marques, and A. C. G. Costa (2013a), Volcano-tectonic evolution of Santa Maria Island: Implications for the Nubia-Eurasia plate boundary in the Azores, *AGU Fall Meeting*, Suppl. Abstract, T51F-2531.

Sibrant, A. L. R., A. Hildenbrand, F. O. Marques, T. Boulesteix, and A. C. G. Costa (2013b), Morpho-structural evolution of a volcanic island developed inside an active oceanic rift: S. Miguel Island (Terceira Rift, Azores), Abstract Meeting, *IAG*, *2013*, Paris, France.

Sibrant, A. L. R., F. O. Marques, and A. Hildenbrand (2014), Construction and destruction of a volcanic island developed inside an oceanic rift: Graciosa Island, Terceira Rift, Azores, *J. Volcanol. Geotherm. Res.*, *284*, 32–45.

Sibrant, A. L. R., A. Hildenbrand, F. O. Marques, and A. C. G. Costa (2015a), Volcano-tectonic evolution of the Santa Maria Island (Azores): Implications for paleostress evolution at the western Eurasia-Nubia plate boundary, *J. Volcanol. Geotherm. Res.*, *291*, 49–62.

Sibrant, A. L. R., A. Hildenbrand, F. O. Marques, B. Weiss, C. Hubscher, T. Ludmann, T. Boulesteix, and A. C. G. Costa (2015b), Morpho-structural evolution of a volcanic island developed inside an active oceanic rift: S. Miguel Island (Terceira Rift, Azores), *J. Volcanol. Geotherm. Res.*, *301*, 90–106.

Sibrant, A. L. R., F. O. Marques, and A. Hildenbrand (2015c), Reply to the comment by Quartau et al. on "Construction and destruction of a volcanic island developed inside an oceanic rift: Graciosa Island, Terceira Rift, Azores", J. Volcanol. Geotherm. Res. 284, 32-45, by Sibrant et al. (2014), *J. Volcanol. Geotherm. Res.*, *303*, 193–198.

Silva, P. F., B. Henry, F. O. Marques, A. Hildenbrand, P. Madureira, A. Mériaux, and Z. Kratinova (2012a), Palaeomagnetic study of a subaerial volcanic ridge (Sao Jorge Island, Azores) for the past 1.3 Myr: Evidence for the Cobb Mountain Subchron, volcano flank instability and tectonomagmatic implications, *Geophys. J. Int.*, *188*, 959–978.

Silva, R., J. Havskov, C. Bean, and N. Wallenstein (2012b), Seismic swarms, fault plane solution, and stress tensors for São Miguel Island central region (Azores), *J. Seismol.*, *16*, 389–407.

Silveira, G., and E. Stutzmann (2002), Anisotropic tomography of the Atlantic Ocean, *Phys. Earth Planet. Int.*, *132*, 237–248, doi:10.1016/S0031-9201(02)00076-6.

Silveira, G., L. Vinnik, E. Stutzmann, V. Farra, S. Kiselev, and I. Morais (2010), Stratification of the Earth beneath the Azores from P and S receiver functions, *Earth Planet. Sci. Lett.*, *299*, 91–103.

Snow, J. E., and H. N. Edmonds (2007), Ultraslow-spreading ridges rapid paradigm changes, *Oceanography*, *20*(special issue 1), 90–101.

Soares, D. M., T. M. Alves, and P. Terrinha (2012), The breakup sequence and associated lithospheric breakup surface: Their significance in the context of rifted continental margins (West Iberia and Newfoundland margins, North Atlantic), *Earth Planet. Sci. Lett.*, *355-356*, 311–326.

Spang, J. H. (1972), Numerical method for dynamic analysis of calcite twin lamellae, *Geol. Soc. Am. Bull.*, *83*(2), 467–472.

Sperner, B., and P. Zweigel (2010), A plea for more caution in fault–slip analysis, *Tectonophysics*, *482*(1–4), 29–41.

Sperner, B., L. Ratschbacher, and R. Ott (1993), Fault-striae analysis: A Turbo Pascal program package for graphical presentation and reduced stress tensor calculation, *Comput. Geosci.*, *19*(9), 1361–1388.

Thibauld, R., P. Gente, and M. Maia (1998), A systematic analysis of the Mid-Atlantic Ridge morphology and gravity between 15°N and 40°N: Constraints on the thermal structure, *J. Geophys. Res.*, *103*, 24,223–24,243, doi:10.1029/97JB02934.

Trota, A., N. Houlié, P. Briole, J. L. Gaspar, F. Sigmundsson, and K. L. Feigl (2006), Deformation studies at Furnas and Sete Cidades Volcanoes (São Miguel Island, Azores). Velocities and further investigations, *Geophys. J. Int.*, *166*, 952–956.

Tucholke, B., J. Lin, M. Kleinrock, M. Tivey, T. Reed, J. Goff, and G. Jaroslow (1997), Segmentation and crustal structure of the western Mid-Atlantic Ridge flank, 25°25′-27°10′N and 0-29 m.y, *J. Geophys. Res.*, *102*, 10,203–10,223, doi:10.1029/96JB03896.

Turner, F. J. (1953), Nature and dynamic interpretation of deformation lamellae in calcite of three marbles, *Am. J. Sci.*, *251*(4), 276–298.

Udías, A., A. Lopez Arroyo, and J. Mezcua (1976), Seismotectonic of the Azores-Alboran region, *Tectonophysics*, *31*, 259–289.

Van Wijk, J. W., and D. K. Blackman (2005), Deformation of oceanic lithosphere near slow-spreading ridge discontinuities, *Tectonophysics*, *407*, 211–225.

Vogt, P. R. (1976), Plumes, sub-axial pipe flow, and topography along the Mid-oceanic ridge, *Earth Planet. Sci. Lett.*, *29*, 309–325.

Vogt, P. R., and W. Y. Jung (2004), The Terceira Rift as hyper slow, hotspot dominated oblique spreading axis: A comparison with other slow spreading plate boundaries, *Earth Planet. Sci. Lett.*, *218*, 77–90.

Walker, G. P. L. (1984), Downsag calderas, ring faults, caldera sizes, and incremental caldera growth, *J. Geophys. Res.*, *89*(B10), 8407–8416, doi:10.1029/JB089iB10p08407.

Wallace, R. E. (1951), Geometry of shearing stress and relation to faulting, *J. Geol.*, *59*, 118–130.

Walter, T. R., and V. R. Troll (2001), Formation of caldera periphery faults: An experimental study, *Bull. Volcanol.*, *63*, 191–203.

Weiß, B. J., C. Hübscher, and T. Lüdmann (2015a), The tectonic evolution of the southeastern Terceira Rift/São Miguel region (Azores), *Tectonophysics*, *654*, 75–95.

Weiß, B. J., C. Hübscher, D. Wolf, and T. Lüdmann (2015b), Submarine explosive volcanism in the southeastern Terceira Rift/São Miguel region (Azores), *J. Volcanol. Geotherm. Res.*, *303*, 79–91.

Wendt, J. I., M. Regelous, Y. Niu, R. Hékinian, and K. D. Collerson (1999), Geochemistry of lavas from the Garrett Transform Fault: Insights into mantle heterogeneity beneath the eastern Pacific, *Earth Planet. Sci. Lett.*, *173*, 271–284.

Whittaker, J. M., R. D. Muller, W. R. Roest, P. Wessel, and W. H. F. Smith (2008), How supercontinents and superoceans affect seafloor roughness, *Nature*, *456*, 938–941, doi:10.1038/nature07573.

Yang, T., Y. Shen, S. Van Der Lee, and C. Solomon (2006), Upper mantle structure beneath the Azores hotspot from finite frequency seismic topography, *Earth Planet. Sci. Lett.*, *250*(1–2), 11–26.

Zandomeneghi, D., J. Almendros, J. Ibáñez, and G. Saccorotti (2008), Seismic tomography of Central São Miguel, Azores, *Phys. Earth Planet. Inter.*, *167*, 8–18.

Zanon, V. (2015), Conditions for mafic magma storage beneath fissure zones at oceanic islands. The case of São Miguel island (Azores archipelago), *Geol. Soc. London, Spec. Publ.*, *422*, SP422. 4.

Zanon, V., and A. Pimentel (2015), Spatio-temporal constraints on magma storage and ascent conditions in a transtensional tectonic setting: The case of the Terceira Island (Azores), *Am. Mineral.*, *100*(4), 795–805.

Zbyszewski, G. (1961), Étude géologique de l'Île de S. Miguel (Açores), *Comun. Serv. Geol. Port.*, *45*, 6–176.

Zbyszewski, G., O. V. Ferreira, and C. Torre de assuncao (1959), *Carta Geológica de Portugal na escala de 1:50 000. Notícia explicativa da Folha A, S.Miguel (Açores)*, *Publ. Serv. Geol. de Portugal*, 22 pp., Lisboa, Ponta Delgada.